Study of Mechanical Properties of Friction Stir Welded Dissimilar Aluminium Alloys

A

Project Repot

Submitted in partial fulfillment of the requirement for the award of the degree of

Master of Technology

in

Production Engineering

by

Kudzanayi Chiteka (2K12/PRD/32)

under the guidance of

Mr. N. Yuvaraj (Asst. Prof.)

DEPARTMENT OF MECHANICAL ENGINEERING

DELHI TECHNOLOGICAL UNIVERSITY

NEW DELHI-110042

JULY-2014

CERTIFICATE

Delhi Technological University

Department of Mechanical Engineering

Delhi-110042

This is to certify that the thesis entitled **'Study of Mechanical Properties of Friction Stir Welded Dissimilar Aluminium Alloys'** done by **Kudzanayi Chiteka** (Roll Number 2K12/PRD/32) on partial fulfilment for the award of degree of Master of Technology in Production Engineering at **Delhi Technological University**, is an authentic work carried out by him under my guidance. The matter embodied in this thesis has not been submitted earlier for the award of any degree or diploma to the best of my knowledge and belief.

Guided by Mr. N. Yuvaraj
Assistant Proffessor
Department of Mechanical Engineering
Delhi Technological University
Delhi-110042

Signature: ……

Date: ……

ABSTRACT

The relatively new joining process of friction stir welding (FSW) is a solid state joining process which does not involve the melting of the base materials. Aluminium alloys AA5083-H32 and AA6061-T6 have been previously joined with other types of aluminium alloys, very little work has been reported on the joining of these two materials by FSW. In this research, dissimilar joints were made using three different tool rotation speeds of 630 rpm, 1000 rpm and 1600 rpm and three traverse speeds which were 16, 20 and 40 mm/min. Three tool configuration were used and these had different pin to shoulder diameter ratios of 2.5, 3.0 and 3.5. Full factorial face centred central composite design was used to minimise the number of experiments done. Response surface methodology was used to optimise the parameters as well as perform regression analysis to determine the inter-relationships between the three parameters used in the joining process. Three different regions namely base material, heat affected zone, thermo-mechanically affected zone and nugget zone have been observed in the weld. The joining process was successful with a tensile strength above 70% of the base material and a fine grained microstructure which was a result of recrystallization.

DEDICATIONS

This research is dedicated to my family; my mother Krezasteji-L and my father Shri Davies Chiteka, my sister Pestalos-C who have supported me all the way since the beginning of my studies.
Also I dedicate this work to Rejoh my fiancé who has been a great source of moral support, strength, motivation and inspiration.

ACKNOWLEDGEMENTS

I am greatly indebted to my mentor Shri N. Yuvaraj for his patience, concern, invaluable guidance and also encouragement throughout the undertaking of this research. I wish to express my gratitude to the Mechanical Engineering Department faculty members, Professor V. Jeganathan, Mr. Pradeep Kr., Mr. Francis, Mr. Sunil, Mr. Tek Chand, Mr. Netram and many others whose support was great for the success of this work and their continued support with the resources and technical knowledge without which this work could not have been possible.

TABLE OF CONTENTS

LIST OF FIGURES

LIST OF TABLES

LIST OF EQUATIONS

Chapter 1

INTRODUCTION

Friction Stir Welding (FSW) technique is becoming a popular method to join aluminium alloys for transportation, marine and aerospace applications [1-3]. These applications need lightweight and high mechanical properties [1]. FSW is a joining process which involve forging and extrusion and not a welding process in true sense [4].

The method of Friction Stir Welding (FSW) was discovered by Wayne Thomas at TWI (The Welding Institute), and the first patent applications were filed in 1991, [5]. Friction Stir Welding is a solid-state process, because the workpieces are joined without attaining melting point of the base metals [6]. The FSW process consists of joint formation happening below the base material's melting temperature. This discovery has opened up for new areas of research in welding technology. With the FSW process, it is now possible to make high quality welds of 2000 and 7000 series alloys, which were previously considered unweldable.

In FSW welding process, a shouldered tool with a profiled pin is rotated and inserted into the joint area between two workpieces of sheet or plate material. The parts are securely fixed to the machine table to prevent the joint faces from being split apart. Frictional heat generated between the FSW welding tool and the work cause the latter to soften though not reaching its melting point, allowing the tool to traverse through the weld line. The plasticised material is transferred to the trailing edge of the tool pin and forged through intimate contact with the tool shoulder and pin profile. A solid phase bond is created between the work-pieces when it cools. Friction Stir Welding can be used to join aluminium sheets and plates, magnesium alloys, copper and steels without filler wire or shielding gas. Initially much focus has been on non-ferrous alloys, but now FSW is being applied to a broad range of materials including steel and titanium. Several similar and dissimilar materials have been joined by FSW. These include, aluminium to aluminium, Titanium and aluminium and aluminium to magnesium. [7-9].

Copper, brass and steels have been successfully joined by this method. Mostly simple welds have been made on the conventional milling machines. However, for more complicated joins there is need to use the FSW welding machine which has been specifically designed for such welds.

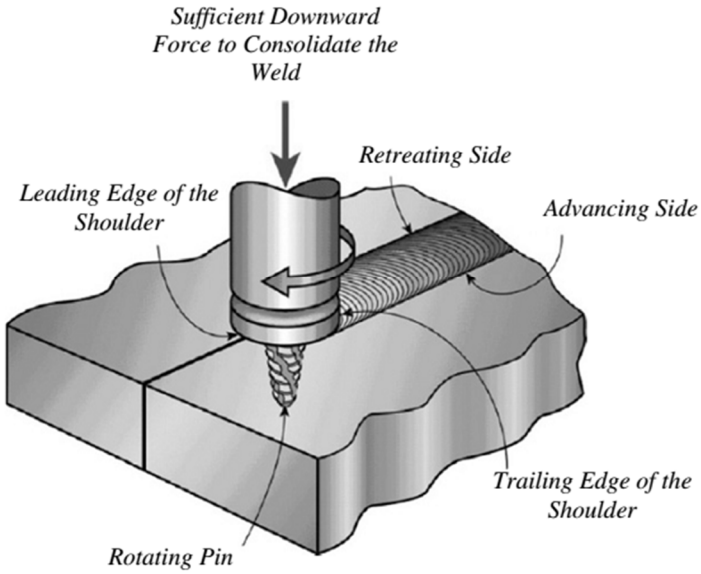

Figure 1. Schematic of friction stir welding [10].

1.1 Motivation

Recent advances in construction and transportation industries where weight reduction is required, aluminium alloys 5083 and 6061 have found a huge application in these areas. These include heavy duty structures in rail coaches, truck frames, ship building, bridges, military bridges, aircraft, piping, pylons and towers, transportation, boiler making; Motorboats, aerospace applications and helicopter rotor skins.

1.2 Key Features of Friction Stir Welding

- Solid state process,
- Low thermal distortion and good dimensional stability,
- No loss in alloying elements,
- Excellent metallurgical properties and fine micro-structure,
- No cracking, porosity and other welding defects,
- Environmental friendly hence called green welding technology,
    - No shielding gas
    - No use of chemical for cleaning
    - No slag and fumes
    - Highly energy efficient

1.3 Advantages

- Good mechanical properties in the as-welded condition.
- Improved safety due to the absence of toxic fumes or the spatter of molten material.
- No consumables — a threaded pin made of conventional tool steel, e.g., hardened H13, can weld over 1 km of aluminium, and no filler or gas shield is required for aluminium.
- Easily automated on simple milling machines — lower setup costs and less training.
- Can operate in all positions (horizontal, vertical, etc.), as there is no weld pool.
- Generally good weld appearance and minimal thickness under/over-matching, thus reducing the need for expensive machining after welding.
- Low environmental impact.

1.4 Disadvantages

- Exit hole left when tool is withdrawn.
- Large down forces required with heavy-duty clamping necessary to hold the plates together.
- Less flexible than manual and arc processes (difficulties with thickness variations and non-linear welds).
- Often slower traverse rate than some fusion welding techniques, although this may be offset if fewer welding passes are required.

The quality of an FSW joint is always superior to conventional fusion-welded joints. A number of properties support this claim, including FSW's superior fatigue characteristics.

1.5 Comparison with Other Welding Techniques

Severe plastic deformation during FSW process at elevated temperature results in the generation of fine and equiaxed recrystallized grains. Good mechanical properties in friction stir welds is a result of fine microstructure produced [11]. FSW has an advantage over fusion processes in that the liquid phase in fusion processes results in problems. These are avoided in FSW. These problems include but not limited to porosity, solidification cracking, solute redistribution and liquation cracking which do not occur in FSW.

FSW technique has the ability to retain the original microstructure and mechanical properties [12]. Grains of similar dimensions as the sub grains are obtained through continuous dynamic recrystallization of the material during the welding process [13, 14].

Mishra (2006) [11] has noted that FSW is associated with less defects we can have variations in parameters and materials but still achieve good weld properties. In fusion welding, certain defects cannot be avoided completely. These include hydrogen embrittlement and liquation cracking. Therefore, it has been shown that since the alloy is not melted during FSW welding process, solid-state welding of aluminium is preferred to other methods. Non-heat-treatable and powder metallurgy aluminium alloys which cannot be joined by fusion welding can now be joined by the FSW process [15].

1.6 Composition and Properties of Aluminium 5083 And 6061 Alloys

AA6061 alloy is known to be high-strength aluminium, magnesium, and silicon alloy in which manganese is added to increase ductility and toughness. On the other hand AA5083 alloy is a light metal alloy with a high degree of corrosion resistance and an excellent balance of mechanical properties. This material is used as a structural material in transportation applications.

Table 1. Summary of the composition, properties and applications of aluminium 6061-T6 and 5083-H32 alloys.

Alloy	**Characteristic properties**	**Applications**
5083	Aluminium 5083 is known for exceptional performance in extreme environments. 5083 is highly resistant to Attack by both sea water and industrial chemical environments. Alloy 5083 also retains exceptional strength after welding. It has the highest strength of the non-heat treatable alloys but is not recommended for use in temperatures in excess of 65°C.	Alloy 5083 is typically used in: Shipbuilding, Rail cars, Vehicle bodies, Tip truck bodies, Mine skips and cages, Pressure vessels.
6061	6061 is a medium to high strength heat-treatable alloy with a strength higher than 6 005. It has very good corrosion resistance and very good Weldability although reduced strength in the weld zone. It has medium fatigue strength. Good cold formability in the temper T4, but limited formability in T6 temper. Not suitable for very complex cross-sections.	Alloy 6061 is typically used for heavy duty structures in: Rail coaches, Truck frames, Ship building, Bridges and Military bridges, Aerospace applications including helicopter rotor, skins, Tube, Pylons and Towers, Transport, Boilermaking, Motorboats and Rivets.

Table 2. Chemical Composition of AA5083-H32 and AA6061-T6.

Component	5083-H32	6061-T6
Al (Wt. %)	92.4 -95.6	95.8 -98.6
Cr (Wt. %)	0.05 -0.25	0.04 -0.35
Cu (Wt. %)	Max 0.1	0.15 - 0.4
Fe (Wt. %)	Max 0.4	Max 0.7
Mg (Wt. %)	4 - 4.9	0.8 - 1.2
Mn (Wt. %)	0.4 - 1	Max 0.15
Si (Wt. %)	Max 0.4	0.4 - 0.8
Ti (Wt. %)	Max 0.15	Max 0.15
Zn (Wt. %)	Max 0.25	Max 0.25

Chapter 2

LITERATURE REVIEW

A survey of the researches which have been undertaken in this research area is outlined in this chapter. The materials which have been joined, similar or dissimilar, metallic or non-metallic will be discussed in relation to the welding conditions and parameters that gave different results. Here a brief discussion is provided and details will be given in the following sub topics.

Traditional aluminium welding methods are associated with defects like porosity and voids, distortion, hot cracking and liquation cracking [4, 16-17]. Proper selection of FSW parameters results in a perfect joint which could be stronger than the base materials. Dickerson and Przydatek [18] discovered that friction-stir-welded butt joints are mostly sound provided process conditions are properly maintained. Process parameters as well as tool geometry are the key factors that influence the soundness of the joint produced [19, 20]. Bahemmat et. al. [19] recognised the importance of tool geometrical parameters which are height, shape, pin and shoulder that affect both the metal flow and the heat generation due to frictional forces developed. Use of the proper tool gives the best results in an FSW weld [2, 13, 21-23]. Traverse speed and rotational speed are factors that need to be taken into consideration when selecting welding parameters since these parameters determine the strength and overall performance of the joint [1, 2, 4, 17, 22, 24-26]. Amancio-Filho et al. [27] joined 2024-T351 and 6056-T4 revealed that the weaker material determines the strength of the joint and similar conclusions were made by Shigematsu [3]. FSW technique has the ability to retain the original microstructure and mechanical properties [12]. Grains of similar dimensions as the sub grains are obtained through continuous dynamic recrystallization of the material during the welding process [13, 14].

2.1 Similar Aluminium Alloys

Rao et. al. (2012) [28] recorded the successful joining of aluminium alloys 5083. It was found that the change in hardness occurred more rapidly at the advancing side (AS) than at the retreating side (RS). They reported a sharp decrease in hardness from the HAZ to the SZ at the advancing side while at the retreating side, this gradient was reported to be small. An asymmetric shape on hardness and micro-tensile profile was attained. Cavaliere et. al. (2008) [29] reported the joining of AA6082. It was noted that increasing the advancing

speed from 40 to 165 mm/min up to a maximum speed of 460 mm/min, a strong variation in the nugget mean grain size was observed. Yield strength was reported to increase with welding speeds up to a speed of 115 mm/min when it started decreasing as the advancing speed increased. The same characteristics were also noted for ductility but, however, after 165mm/min it started increasing again.

Aluminium alloys which have been previously studied have been outlined by researchers, [7, 30-38]. Other results of the work done and the results are displayed in Table 3.

2.2 FSW of Dissimilar Aluminium Alloys and FSW of Aluminium to Other Alloys

At the present time, FSW has mainly been used for joining similar materials. For dissimilar welding, intensive studies are being undertaken aimed at determining the effect of material combination and welding conditions on weld properties. FSW of dissimilar materials will be a requirement in the near future for advanced aircraft design [3]. As such a research conducted in the FSW of aluminium alloys 6061 and 5083 and the materials were joined successfully. The joints were made perpendicular to the rolling direction. A 10 mm shoulder diameter was used together with rotational speeds of 890 rpm and 1540 rpm and traverse speeds of 118 mm/min and 155 mm/min. The joints made of AA5083-AA5083, AA6061-AA6061 and AA5083-AA6061 material combinations produced joint strengths of 97%, 63% and the dissimilar joint was reported to be almost similar to that of AA6061-AA6061 joint. It was concluded that the strength and properties, which include hardness distribution and the tensile strength, were strongly dependent on the material combination of the joint whether similar or dissimilar.

Palanivel et. al. (2012) [2] studied the tensile behaviour microstructure and mechanical properties of 6 mm thick dissimilar aluminium welding of AA6351-T6 alloy to AA5083-H111 alloy produced by friction stir welding using a high carbon high chromium steel tool. Rotation speed was varied amongst 600, 950 and 1300 rpm. Five different tool pin profiles were identified i.e. Straight Square (SS), Tapered Square (TS), Straight Hexagon (SH), Straight Octagon (SO) and Tapered Octagon (TO), with three different welding speeds (50, 63and 75 mm/min) were used to weld the joints. The effect of welding speed and pin profiles on the tensile properties were studied and it was found that the straight square pin profile with 63 mm/min produced better tensile strength than the other tool pin profiles and welding

speeds. The joint which was fabricated using tool rotational speed of 950 rpm and straight square pin profile had the highest tensile strength of 273 MPa.

Karthikeyan et. al. (2012) [39], performed FSW welding of AA 2011 and AA 6063 aluminium alloys, a high speed steel tool hardened to RC-65 and comprising a right handed threaded pin of diameter 6 mm, length 5.9 mm, and a shoulder of 18mm was used. It was observed that welding strength improves with increased tool rotation speed. Optimum tool rotational speed for defect free nugget zone was found to be 1400 rpm and tool feed was found to be 60 mm/min.

Lee et. al. (2003) [26], carried out a research on Cast A356 Al alloy and wrought 6061 Al alloy 4 mm in thickness. The dissimilar formed wrought 6061 Al and A356 Al alloys were successfully joined by the FSW and showed no porosity and defects in both weld top and rear surfaces regardless of the welding conditions.

Khodir and Shibayanagi (2007) [40] examined AA2024 and AA7075 aluminium alloys 3 mm thick using tool steel (SK D61). A sound weld was obtained at rotation speed of 1200 rev/min and welding speed of 1.67 mm/s (100mm/min) when 2024 Al alloy plate was located on the advancing side.

Amancio et. al. (2007) [27] carried out a study on AA2024-T351 and AA6056-T4 with 5mm thickness using a modular FSW tool with 5 mm diameter threaded cylindrical pin and 15 mm concave shoulder. Defect-free friction stir welds were produced for the dissimilar alloy system. Rotational speed of 800 rpm and welding speed of 150 mm/min provided the best results. Results of the researches which have also been done in this area are listed in Table 4.

2.3 Similar and Dissimilar FSW of Magnesium, Steel, Copper, Titanium, Plastics and Other Materials

Beside aluminium alloys other similar materials have been successfully joined and these include carbon steels. Fujii et. al. (2006) [22] recorded the joining of Carbon steel (IF steel, S12C, S35C). It was reported that the strength of the S12C steel joints increases with the increasing welding speed and the strength of the S35C steel joints revealed a peak near 200 mm/min.

Pure copper C11000 has also been joined [41], and the acceptable temperatures for a successful FSW process were found to be between 460 ^{o}C and 530 ^{o}C. It was also observed that the temperatures on the advancing side were found to be slightly higher than those on

the retreating side. The tensile strength and the hardness at the Thermo-Mechanically Affected Zone (TMAZ) were found to be about 60% of the base metal. It was reported that the elongation can go as high as three times that of the base metal, if there is an appropriate temperature control.

Dissimilar joins have also been made between ZK60 magnesium alloy and titanium, 5754AA and C11000 copper, Al 6013-T4 to X5CrNi18 -10 stainless steel. Other materials which have been joined include though not limited to Titanium Ti–6Al–4V, Magnesium AZ31, Plastics have also been reported to have been joined successfully [10, 42-46].

The tables that follow will give the main characteristics of the joints that have been made to date. SD-shoulder diameter; PD-Pin diameter; PL-Pin length; TP-Taper Pin; BD- Base Diameter; TD-Tip diameter; TC-Threaded Cylindrical; TT-Threaded Taper; RPM-rotational speed; TS-Traverse speed; TA-Tilt Angle, SS-straight square; SC-Straight Cylindrical; F-Force;

Table 3. List of materials, tools used, process parameters and the conclusions made on FSW of various similar aluminium alloys.

S/N	Author	Materials Used	Tool Materials	Parameters	Notable Results
1	Venkateswarlu et. al. [47]	AA7039 6mm thickness	Stainless steel tool grade 310. SD-22, 19, and 16 mm. PD-8, 7, and 6 mm.	RPM-710 rev/min & TS- 20 mm/min	Tensile strength was dependent on PD. 7 mm PD produced better results than 6 and 8 mm. SD is not as significant as PD to weld properties.
2	Hao et. al. [48]	Cold-rolled plates of Al–4.7Mg–0.6Mn–0.1Zr–0.3Er (wt%). 3.7 mm thick	TC Steel tool. SD-12 mm. PD-5 mm. PL- 3.4 mm	RPM- 400 – 1200 rpm. TS -100 – 400 mm/min. TA- 2.51^{o}	Defect free joints excluding joint made at 800 rpm with 400 mm/min TS. Equiaxed recrystallized grains in the NZ and the grain size increased with increasing the RPM or decreasing the TS. At speed of 400 rpm with 100 mm/min traverse there was greatest ultimate tensile strength (UTS) of 346 MPa and yield strength (YS) of 218 MPa with a joint efficiency of 73%.
3	Chaitanya et. al. [49]	Al–Zn–Mg aluminum alloy AA7039, 5mm thick	Die steel tool. Truncated conical pin with left hand thread of 1 mm pitch. SD-16mm. BD- 6mm TD-4mm. PL-4.7 mm.	TS- 75 mm/min. RPM- 635 rpm. TA-2.5^{o}	The size of α aluminum grains is increased by post weld heat treatments in all zones of friction stir weld joints. The highest mechanical properties were attained in naturally aged joints with tensile strength 94.9% and elongation 174.2% while solution treated joints had lowest mechanical properties of the joints.
4	Palanivel et. al. [50]	AA5083-H111 aluminum alloy	HCHCr tool , SS, SD-18 mm. PD-6 mm. PL-5.6 mm.	RPM- 500, 750, 1000, 1250 & 1 500 rpm. TS- 30, 49.5, 69, 88.5 & .108 mm/min	Speed of 1000 rpm and a welding speed of 69 mm/min provided higher tensile strength compared to other joints. Tool rotational speed, welding speed and axial force are the parameters affecting the tensile strength of the welds.

5	Parida et. al. [51]	Commercial grade Al-alloy 6mm thick	SS310 tools. SD- 35mm. PL- 6mm. TP Cylindrical	Rotational speed, 1400 rpm. Welding speed, 112mm/min Plunge force, 6300N	Good quality welds were achieved. Tensile strength is more than base material. Lower hardness values implying better ductility. Refined grains within the weld zone.
6	Rao et. al. [28]	Cold rolled H-temper A5083 alloy. 3mm thick	D- 12 mm concave TP, PD- 5 mm	RPM-1800 TS-1000 mm/min F-9.5 kN	Rapid hardness change in the AS compared to the RS. Sharp decrease in hardness from the HAZ to the SZ at the AS. However this it was not sharp in the RS.
7	El-Danaf et. al. [32]	Commercial 6082-T651 AA plates- 6 mm thick,	Mo–W tool steel SD-15mm. PD- 6 mm, PL- 5 mm	RPM- 850, 1040 & 1350 rpm. TS- 90, 140, 224 mm/min	Softening occurred in the SZ and TMAZ. This could be partially recovered by Post Weld Heat Treatment. The grain sizes for all welding conditions were ranging from 2.3 to 2.8 µm.
8	Dong et. al. [35]	6005A-T6 3 mm thick	Cr12MoV tool SD- 12 mm. PD- 3 mm.	RPM- 1200 rpm. TS- 100 mm/min. TA- 2.5^{o}. Plunge depth, 0.1 mm	Tensile properties increased with increasing speed. Joint efficiency attained between 71% and 80%. Fine equiaxed grain structure in the NZ.
9	Yoon et. al. [36]	A5052-O 2 mm thick	SD-10 mm. PD- 4 mm PL-1.7mm	RPM- 2000 & 3000 TS-100 to 900 TA- 3^{o}	Smooth defect-free welds except for RPM of 3000 and TS of 100 mm/min. Grain size in SZ was always smaller than BM. SZ had higher hardness than BM. Tensile properties were similar to BM besides those welds at 3000 rpm and 100 mm/min. The welds had less elongation than the base metals.

10	Heidarzadeh et. al. [24]	AA 6061-T4 plates 4 mm thick	SS pin profile	RPM-763, 900, 1100, 1300 & 1436 TS- 46, 60, 80, 100& 113 mm/min. F-5.32, 6, 7, 8 & 8.68 kN.	Maximum tensile strength was obtained at the following parameters; 920 rpm, 78 mm/min and 7.2 kN, maximum tensile elongation was attained at 1300 rev/min, 60 mm/min and 8 kN.
11	Babu et. al. [33]	Al–Cu–Mg alloy AA2014 sheets 3 mm thick	H13 tool steel. Tri. & TT Cyl. SD=15 mm. PD- 5mm Equilateral Tri. Sides- 5.25mm. TT with 1mm pitch, BD-5mm, TP -4mm	RPM- 500 to 1800 Plunge depth of 5.1 to 5.3 mm, TS-20 to 60 mm/min, TA-1^{o}	FSW lap joints have higher shear strength compared to reverted joints. 19.5kN and 16.5 kN have been attained by triangular and threaded taper cylindrical tools compared to 3.4kN for reverted joints.
12	Ahmed et. al. [34]	AA2017A-T 451 20 mm thick	SD-40mm scrolled TT- Triflat, PL - 19.5mm	RPM- 300 rpm, TS- 120 mm/min TA-2°	Weld efficiency up to 90% on tensile properties. Fracture occurred at the NZ/TMAZ interface during tensile tests which is the softened region in terms of hardness.
13	Costa et. al. [31]	Heat treated AA6082-T6 4 mm thick	TC, SD- 16 mm PD- 5 mm	TS- 300 mm/min, TA-2^{o} RPM 1500	Fatigue life reduction due to tunnel defects and shear lips. Tunnel defects are more detrimental to fatigue resistance than stress concentration created near shear lips.
14	Liang et. al. [52]	2519-T87 aluminum alloy 10mm thick	SD- 20 mm coniform threaded pin, PD- 10 m, PL- 9 mm	RPM- 250 TS-30 mm/min	Weld nugget experienced dynamic recrystallization and resulted in the size of recrystallized grains being smaller than that in the TMAZ affected zone.

15	Zhang et. al. [53]	2024-T3 Al thickness of 1.6 mm	3 types of flute shoulders; i.e. inner-concave, concentric circles and three spiral flute shoulder	TS- 20 mm/min RPM-1800 rpm	Uniformity of grains was better with 3-spiral-flute shoulder. Good corrosion resistance at TS of 20 mm/min RPM of 1800 rpm & tensile strength of 80% more than that of parent metal could be achieved.
16	Gaafer et. al. [38]	AA7020-O wrought Al alloy 12mm thick	H13 steel PD- 5 mm SD-35 mm PL-8 mm	TA- 3^o rotational RPM- 1120, 1400, & 1800 rpm, TS- 20, 40 and 80 mm/min	Increasing TS increases hardness at the weld zone. Increasing TS has no influence on hardness at the NZ at 1120 and 1400 rpm. Ductility increases with increasing the RPM.
17	Cavaliere et. al. [29]	AA6082 commercial aluminium 4 mm thick	PD- 6.0 mm PL- 3.9 mm SD- 14 mm	RPM-1600 TS- 40, 56, 80, 115, 165, 325 &460 mm/min TA- 3^o	Yield strength was increased strongly from the lower speeds up to 115 mm/min after which it started to decrease by increasing the advancing speed. Ductility of the material followed the same behaviour but restarted to increase after 165 mm/min
18	Ren et. al. [54]	6 mm thick 6061Al–T651 rolled plate	TC, SD- 24 mm PD- 6 mm	RPM- 400, 600, 800, 1200 & 1600 TS- 100 & 400 mm/min.	Welding speed of 400 mm/min resulted in higher tensile strength with 40^o shear fracture. Speed of 100mm/min provided inferior results.
19	Wei et. al. [55]	01420 Al–Li alloy 2mm thick	1Cr18Ni9Ti stainless steel. Tapered. SD-9mm. TD- 2mm BD- 2.6 mm,	TA- 2^o RPM-480, 600, 930, 1370 & 1960 TS- 23.5, 39.1, 54.5, 72 & 85.7 mm/min, F-1000 and 7000 N	Joint UTS was 86% of BM and the maximum bending angle of the joints could reach 180^o. Welding pressure increased with the increase in the TS or the decrease in the RPM. SZ had higher hardness values than BM.

20	Marzoli et. al. [56]	AA 6061, precipitation hardenable. Reinforced with 20% volume Al2O3 (alumina) particles. 7mm thickness	Ultra-hard tool material. SD-20 mm. PD-8 mm	RPM- 100 to 700rpm. TS- 100-500mm/min.	The reinforcement particles distribution and shape is affected by the stirring effect of the tool. Joint efficiencies between 70% and 80% have been revealed through tensile tests.
21	Cavaliere et. al. [57]	AA6056 commercial aluminium alloy 4 mm thick	PD- 6.0 mm PL-3.9 mm SD- 14 mm	TS- 56 mm/min. TA-3◦ RPM- 500, 800 & 1000	Highest values of ductility were attained at 40 and 56 mm/min & a rotating speed of 500 rpm and it decreased with increasing speed. Highest RPMs of 800 and 1000 rpm and the highest TS used i.e. 80 mm/min produced the highest tensile strength.
22	Peel et. al. [37]	AA5083 3mm thick	SD-18 mm; M5 and M6 threaded pin, PD- 5mm, 0.8 mm pitch	TS- 100, 150, 200, mm/min with M5 tool & another at 200 mm/min with M6 tool. TA-2°	Lower hardness as a result of recrystallization in the weld zone. Plastic flow during tensile testing occurred within the recrystallized zone of the weld. Longitudinal stresses increased win increase in traverse speed.

Table 4. List of materials, tools used, process parameters and the findings made on FSW of various dissimilar aluminium alloys and also between aluminium alloys and other materials.

S/N	**Author**	**Materials Used**	**Tool Materials**	**Parameters**	**Remarks**
23	Venkateswaran et. al. [58]	Extruded 6063-Al (T5) and rolled AZ31B-Mg (H24). 3.25 mm thick	H13 tool steel. SD-18mm, PD-5mm fluted probe of cobalt base super alloy (MP159).	RPM- 900–2700 TS- 1.69–6.4 mm/s. F-14–30 kN. TA-1^{o} and 3^{o}.	NZ grain size increase as tool rotation speed increase. Different microstructural phases were present in the NZ and hence there was fluctuating micro-hardness. Tensile strength of joint is 68% of the 6063-T5 base metal with a maximum elongation of 1%.
24	Palanivel et. al. [2]	AA5083-H111 and AA6351-T6. 6mm thick	HCHCr, 63 HRC. SD- 18mm. PD-6mm. PL-5.7 mm. Pin profiles, SS, SH, SO, TS, and TO.	RPM- 600, 950, 1300 TS- 60mm/s F- 8kN TA- 0^{o}	The joints fabricated using straight tool profiles had no defects while tapered tool profiles caused a tunnel defect at the bottom. Square pin profiled tool at TS of 63 mm/min showed the best tensile properties. Strength of 273 MPa was attained.
25	Akinlabi et. al. [43]	5754 AA and C11000 copper 3.175 mm thick	H13 tool 52 HRC. SD-15, 18 & 25mm PD- 5 mm.	RPM 600 to 1200 TS-50 & 300mm/min. TA-2^{o}	Tensile strength is affected by the downward force exerted by the machine. The optimal conditions for high tensile strength was achieved at 950 rpm and 150 mm/min.
26	Dinaharan et. al. [59]	AA6061 cast and wrought, 6 mm thick.	HCHCr, 62 HRC Hex. profile. SD-19.2 mm, PD-6mm PL-5.8 mm.	RPM- 800 to 1400 TS 50 mm/min, F-8 kN TA-0^{o}	The microhardness of some portion of weld zone was higher than other areas. Maximum tensile strength was attained when cast aluminium alloy was placed in the advancing side at 1200 rpm.
27	Koilraj et. al. [60]	Al–Cu alloy AA2219-T87 and Al–Mg	H13 tool. Straight Cyl. Taper Cyl. Cyl. threaded, TT. PL-	Straight Cly,400rpm & 15 mm/s. Tapered Cyl, 550rpm 30mm/s.	Joint soundness is determined by the ratio between tool shoulder diameter and pin diameter. Welding

		alloy AA5083-H321 plates. 6mm thick	5.7 mm PD- 6 mm.	Cyl threaded 700rpm - 45mm/s. TT, 800 rpm -60mm/s.	speed and pin geometry also have a role to play. Lowest hardness values were detected in the HAZ.
28	Xia-wei et. al. [61]	Commercially-available pure copper and 1350 AA sheets with a thickness of 3 mm	SD-16mm Concaved. TT, PD-5.2 mm dia. PL-2.75 mm	RPM- 1000 TS- 80 mm/min. TA- 2.5°	The RPM of 1000 and TS of 80 mm/min produced sound welds. The NZ had a complicated microstructure in which vortex-like pattern and lamella structure were found. Hardness at the copper side of the nugget is higher compared to the aluminum alloy side. The ultimate tensile strength was 152 MPa and elongation of 6.3% was attained.
29	Karthikeyan et. al. [39]	AA2011 and AA6063 10mm thick	HSS tool. RH threaded. PD- 6mm, PL- 5.9mm, SD-18mm.	TS- 40, 60 & 80 mm/min. RPM- 1200, 1400 & 1600 rpm	Defect free welds at 1400rpm. The optimum tool feed was 60 mm/min.
30	Ogura et. al. [62]	A3003-H112, 15 mm thick & SUS304 (SS) 12 mm thick	W-C tool threaded probe, PD-7 mm.	RPM- 900 rpm, TS-300 mm/ min. TA-1.5^{o}	Tensile strength at the NZ and on the AS was larger than that on the RS. Fracture occurred in the A3003 matrix in the specimen.
31	Kumbhar et. al. [63]	A5052 & A6061 5mm thick	HSS tool, PL- 4.8 mm. PD- 6mm. SD-25mm	TA- 3^{o}. RPM-1120 & 1400 rpm. TS- 60, 80 & 100 mm/min.	Abrupt change in microhardness across the interface of the nugget. Tensile properties of the FSW AA5052-AA6061 specimens were better than of individual FSWed Materials

32	Wei et. al. [64]	A1060 & Ti alloy Ti–6Al–4V 3 mm thick	W-C with concave shoulder. SD- 25 mm. PD-6 mm. PL-3.2 mm	RPM- 950. TS-150, 235, 300, 375 & 475 mm/min. TA - 0°	A visible swirl-like mixed region existed at the interface. The ultimate tensile shear strength of joint attained a value of 100% of 1060Al that underwent thermal cycle provided by the shoulder.
33	Xue et. al. [65]	A1060 & pure copper (99.9% purity) 5mm in thick	Heat-treated tool steel. SD- 20 mm in dia. PD- 6 mm. PL-4.8 mm	RPM- 400–1000. TS-100 mm/min. Pin offsets from 0 mm to 3 mm	Defect free joints were obtained at large pin offsets with Cu at the AS. Good Tensile properties have been attained at higher RPM rates and pin offsets of 2 and 2.5 mm. The joint produced at 600 rpm with a pin offset of 2 mm could be bended to 180^{o}.
34	Esmaeili et. al. [66]	Aluminum 1050H16 to brass (70%Cu–30%Zn). 3mm thick	Alloy steel 45HRC. SD-15mm. Tapered slotted pin. BD-5 & TD-4mm	TS- 8 mm/min. RPM-200, 450, 650 & 900 rpm. TA- 1.5^{0}	Maximum tensile strength of 80% of the base metal was attained. When optimum parameters are used defect free welds can be produced. Severe mechanical twining was reported in TMAZ of brass which cause high values of hardness in this region.
35	Bahemmat et. al. [67]	AA7075-T6 and AA6061-T6 5mm thick	TT tool pin profile.	RPM- 900 rpm. Penetration -0.3 mm. TS-80, 100, 120 &160 mm/min. TA-2◦	Average hardness in SZ increases with TS. Superior ultimate stress owing to the higher hardness and strength of the HAZ.
36	Ghosh et. al. [17]	A356 and 6061 3mm Thick	HSS tool. SD- 15 mm, PD- 5 mm PL- 2.6 mm.	RPM-1000–1400 rpm TS- 80–240 mm/min F- 5 kN, TA- 3^{o}	Joint fabricated using lowest TS and RPM, exhibits substantial improvement in bond strength i.e. 98% of that of 6061 alloy, which is also maximum with respect to others.

37	Saeid et. al. [68]	AA1060 4mm thick and commercially pure copper 3mm thick	Quenched and tempered steel tool. SD-15 mm, LH threaded, PD- 5mm, PL-6.5 mm	RPM- 1180 rpm TS- 30, 60, 95, 118, 190, 300 & 375 mm/min. TA- 3^{o}	TS of 95 mm/min provided maximum tensile and shear strength. Cavity defects were produced at higher TS of 118 and 190 mm/min.
38	Brown et. al. [69]	7050-T7451 Al plate 6.4 mm thick	Two-piece design, H13 tool, SD- 17.8 mm single scroll shoulder. MP-159 probe truncated cone 8^{o} taper with threads and three flats. PL- 6.1 mm, PD-7.9 mm at the intersection with the shoulder.	RPM- 540 rpm. TS-6.77 mm/s.	Processing at low tool rotation and traversing speed result fine grain size of 6061 alloy near interface. Lowest tool rotational and traversing speed exhibits superior mechanical properties with respect to the others
39	Tanaka et. al. [70]	Mild steel & A7075-T6 3mm thick	Threaded, PD- 4mm, SD- 12 mm, PL- 2.9 mm	RPM- 400–1200 rpm TS-100 mm/min	No joint failed in the aluminium BM during tensile tests.
40	Moreira et. al. [16]	6061-T6 & 6082-T6 3 mm thick	M5 threaded. 7^{o} smooth concave Shoulder. SD-17 mm	TS- 224 mm/min; TA- 2.5^{o}, RPM- 1120 rpm.	Lower yield and ultimate stresses of the welds. In tensile tests, failures occurred near the weld edge line where a minimum value of hardness was observed.

41	Kwon et. al. [71]	AZ31B-O and A5052P-O alloy plates. 2mm thick	SD-10 mm. PD- 4 mm and PL- 1.7 mm	RPM 800 to 1600 rpm. TS-300 mm/min	RPMs of 1000, 1200, and 1400 rpm, Produced defect-free welds. Better surface appearance as RPM was increased. Maximum tensile strength of 132 MPa was attained at RPM of 1000. There was elongation of 2% or less, regardless of the RPM.
42	Cavaliere et. al. [72]	AA6082–AA2024 4 mm thick	Threaded C40 steel tool. Tapered, BD-3.8 mm & TD-2.6 mm, SD- 9.5 mm	TS- 80 &115 mm/min RPM- 1600 RPM	The best tensile and fatigue properties were obtained for the joints with the AA6082 on the advancing side and welded with an advancing speed of 115 mm/min.
43	Amancio et. al. [27]	AA2024-T351 and AA6056-T4 5mm thickness	Modular tool, PD-5mm threaded cyl. SD- 15 mm	RPM- 800 rpm. TS- 150 mm/min	Defect-free friction stir welds were produced.
44	Khodir et. al. [40]	AA2024 and AA7075 3 mm thick	Threaded Tool steel SKD61. SD- 12 mm. PD-4 mm	RPM-1200 rpm. TS-0.7, 1.2, 1.7 & 3.3 mm/s.	The rise in TS tended to the formation of kissing bond and pores especially when the 2024 Al alloy plate was located on the retreating side
45	Khodir et. al. [73]	2024-T3 Al alloy and AZ31 Mg alloy of plates. 3 mm thickness	Threaded SKD61. SD- 12mm. PD- 4 mm	RPM- 2500 rpm. TS-200, 300, 400 & 550 mm/min. TA- 3^{o}	Increasing TS resulted in redistribution of phases in SZ where the regions occupied by 2024 Al alloy concentrated in the lower portion of SZ while AZ31 Mg alloy concentrated in the upper region beneath the tool shoulder.
46	Vural et. al. [15]	EN AW 2024-0 and EN AW 5754-H22 Al. 3mm thickness	M6 threaded Pin SD- 18mm. PD-6mm, PL-2.8mm	RPM-1000, TS-20 mm/min	Welding performance of ENAW 2024-0 reached 96.6 %. No significant hardness increase after the welding process.

47	Steuwer et. al. [74]	Non-age-hardenable AA5083 and age-hardenable AA6082 alloys 3 mm thick	Pentagonal pin SD-18mm, PD- 6 mm M6 thread (0.8 mm pitch).	100mm/min at 280 rpm, 200 mm/min at 560rpm,& 300mm/min at 840 rpm	Increasing the RPM will also increase the size of the tensile residual lobes on either side of the weld line.
48	Prime et. al. [75]	7050-T7451 and 2024-T351 Aluminium alloys plates 25.4 mm thick	Threaded-pin tool.	TS- 50.8 mm/min.	Very low residual stresses were encountered, even in FSW of thick, dissimilar, high strength aluminium alloys.
49	Cavaliere et. al. [7]	2024 and 7075 Al alloy 2.5mm thickness	PD- 6 mm. PL-2.5 mm. SD-20 mm	TS- 2.67 mm/s TA- 3^{o}	The presence of the FSW line reduces the fatigue behaviour but the comparison to the parent materials is acceptable and allows considering the FSW as an alternative joining technology for the aluminium sheet alloys.
50	Uzun et. al. [44]	Al 6013-T4 To X5CrNi18 -10 stainless steel 4 mm thick		RPM- 800 rpm TS- 80 mm/min	Study has revealed that Al 6013 alloy can be joined to dissimilar stainless steel. The hardness value at the retreating side sharply decrease towards the weld nugget from the level of the TMAZ in the stainless steel at advancing side of weld
51	Jiang et. al. [76]	A6061-T6 & cold-rolled sheet AISI 1018 mild steel 6mm Thick	H13 tool. SD-25 mm, PD- 5.5 mm	RPM- 914 rpm. TS-140 mm/min	Defect free weld was produced. The joint had higher hardness and strength than the base material.

52	Lee et. al. [26]	Cast A356 and wrought A6061 4 mm thick.		TS-87 to 267mm /min. RPM-1600. TA- 3^{o}	Maximum tensile strength of the joints of 423 MPa was achieved at a welding speed of 1.7 mm/s
53	Shigematsu et. al. [3]	5083 and 6061 3 mm thick	SD-10 mm. PD- 3.0 mm. PL- 2.8mm	RPM- 890 & 1540 rpm. TS- 118 & 155 mm/min.	FSW of the similar materials 5083 and 6061 aluminium alloys and dissimilar materials 6061/5083 was carried and it was reported that every combination of materials was joined successfully.
54	Ouyang et. al. [77]	6061-Al and 2024-Al alloy plates of 12.7 mm thickness	Tool steel	RPM-151-914 TS-57-330 mm/min	As the RPM becomes faster, the mechanical mixing of the material in the dissimilar welds becomes more uniform.
55	Madhusudhan et. al. [78]	AA 6262-T6 and AA 7075-T6 6mm thick plates.	H13 tool steel. Cylindrical pin. PD- 6mm. SD- 18mm	RPM-1000, 1200, 1400 rpm. TS-0.4, 0.6 ,0.8 mm/sec. F- 8, 9, 10 kN SD-18 mm. PD- 6, mm. PL- 5.8 mm	Better mechanical properties were obtained at 1200 rpm and 0.6 mm/sec weld speed and 9kN axial force. The SZ region shows a new equiaxed fine grain structure compared to the base metals

Table 5. List of materials, tools used, process parameters and the findings made on FSW of various materials besides aluminium alloys.

S/N	**Author**	**Materials Used**	**Tool Materials**	**Parameters**	**Notable Achievements**
58	Khodaverdizadeh et. al. [79]	Commercial pure copper plate with a thickness of 5 mm	Threaded cyl & sq. pin profiles. PD-6 mm. SD-20 mm. PL- 4.7 mm	RPM- 600 rpm. TS-75 mm/min	Finer recrystallized grain structure and higher mechanical properties for square pin profile relative to sample welded by threaded cylindrical profile.
59	Liu et. al. [80]	ZK60 and AZ31 magnesium alloys. 6mm thick	SD- 15mm. PD- 5 mm, thread pin, PL- 5.45 mm.	TA- 2.51^{o}. RPM- 800 rpm. TS- 100mm/min	No defects were reported. SZ had refined grains and the ultimate tensile strength of the joints was found to be 78–82% of AZ31 base metal.
60	Choi et. al. [81]	AZ31 with CaO Mg alloys. 3.5 mm thick	SKD11 tool. SD- 20 mm. PD-6 mm PL-9 mm.	RPM 1600 rpm, TS- 80 mm/min. TA- 3^{o}.	SZ was found to be harder than the BM, probably due to the presence of fine grains and thermally stable intermetallic compound. Increase in the hardness of the SZ has been attributed to stable intermetallic compound.
61	Wang et. al. [82]	Oxide dispersion strengthened alloy MA956, 3.4 mm thick	Hybrid tool, WC-Co face & W-Ni-Fe shank. SD-10 mm concave. 1.1 mm tapered pin, BD-4.5 mm, TD- 3 mm	RPM- 1000 rpm. TS- 0.85 mm/s. Plunge depth -1.27 mm, TA- 3^{o}. Argon shielding was used	There was fine grained microstructure. Tensile behaviour almost similar to BM. There was 145 MPa tensile strength enhancement without loss in ductility.

62	Galvão et. al. [83]	Deoxidized copper (copper-DHP), temper class R240, 1 mm thick	PD- 3 mm. PL-0.9 mm RH thread. SD-3 mm-dia. 6^{o} conical concave	RPM- 400-1000rev /min. TS-160- 250 mm/min	Many defects were produced for all welding conditions using flat shoulder. Scrolled shoulder tool is better than the conical shoulder in the production of defect free welds, but both geometries required a minimum rotational speed to avoid internal defects.
63	Esmailzadeh et. al. [84]	Lean duplex stainless steel, 1.5mm thickness	WC-base tool. SD-16. PD-4mm, PL-1.25mm,	RPM- 800 rpm TS-50, 100 &150 mm/min. TA-3^{o}. Argon shielding with flow rate 20 *l*/min	When TS was increased, there was a decrease in the peak temperature and the grain size of the ϒ in the weld zone, and thus, improved hardness value and tensile strength of the stir zone.
64	Bagheri et. al. [10]	Acrylonitrile butadiene styrene (ABS) Thermoplastic.	CK45 Threaded tool. PD-10 mm. 7 mm pitch. PL-19 mm pin. SD-17mm	RPM- 800, 1250 &1600 rpm. TS-20, 40 & 80 mm/min. Shoe temperature 50, 80 and 100^{o}C	Weld quality is increased when welding at a high level of RPM and shoe temperature. Weld tensile strength is increased by a lower level of tool travel speed.
65	Aonuma et. al. [42]	ZK60 magnesium alloy and titanium 2mm thick	SKD61 Threaded, SD- 15mm, PL-1.9 mm, PD-6.0 mm	RPM- 850 rpm. TS-50 & 100mm/min F- 7.8KN TA- 3^{o}	The average tensile strength of the joint was 237MPa, which was about 69% of that of ZK60 and a fracture occurred mainly in the stir zone of ZK60 and partly at the joint interface. A thin Zn and Zr-rich layer with about 1mm in thickness was formed at the joint interface, which affected the tensile strength of the dissimilar joint of ZK60 and titanium.

66	Commin et. al. [46]	AZ31-O Magnesium alloy, 2mm thick	PD-5 mm. 2 different SD (10 & 13 mm)	RPM- 1000 rpm TS- 200 mm/min. F- 6.5 – 6.8 kN	The final mechanical properties were dependent on the induced residual stresses. The TMAZ had higher residual stresses especially on the advancing side. yield stress was lower than BM.
67	Ahn et. al. [85]	409L ferritic stainless steel 3.0 mm thick.	Silicon nitride Si3N4 tool. SD-20mm Convex shoulder. Tapered Cyl, PL-2mm. BD-5mm, TD-3mm	RPM- 700 TS-60 mm/min TA- 1^{o}	The stir zone (SZ) had equiaxed grains with ferrite structures due to dynamic Recrystallization. No defects were observed in the stir zone. Equiaxed ferrite grain structure was observed in the SZ. Same corrosion properties of welds compared to base material.
68	Khodir et. al. [86]	Plates of SK4 high carbon steel alloy (0.95% C). 2 mm thick	WC-base tool. SD-12 mm PD-4 mm	RPM-100 to 400 TA- 3^{o} TS-100 mm/min Argon shielding gas	At 100 rpm, there was formation of duplex structure of spheroidal cementite and fine ferrite and it was homogenously distributed in the entire SZ. At higher than 100rpm fine pearlite and martensite structures were formed in the upper part of the SZ and increased with the increasing rotation speed.
69	Sato et. al. [87]	Zircaloy-4 of nuclear grade. 3.1 mm thickness	Co-based alloy tool. SD-15 mm. PL-1.7 mm. Tapered, BD-6 mm TD-3.5	RPM- 150 rpm TS-100 mm/min. TA- 3^{o}	FSW was successful in joining Zircaloy-4. A shiny, smooth surface was attained. Defect-free welds with a fine equiaxed grain structure in the stir zone were obtained but it had an increase in hardness.
70	Jafarzadegan et. al. [88]	3 mm-thick plates of 304 austenitic stainless steel	WC–Co tool. SD-16 mm, PD-5.5 mm.PL -2.6 mm	TS- 50 mm/min RPM- 400 and 800 TA-3°. Argon gas shielding	Sound welds were made between the st37 and 304 steel plates. These welds were basin shaped in the cross-section. Four different microstructures were registered in the welds, except the two base

		were butt-jointed to plates of st37 steel			materials. The HAZ in st37 steel side displayed partially and fully refined microstructures like fusion welding processes. Recrystallization improved the hardness.
71	Chung et. al. [89]	Hyper-eutectoid steel (0.85mass% C, AISI-1080), 1.6 mm thick	WC-based tool. SD- 12 mm PD- 4 mm PL- 1.5 mm.	RPM- 100&400 TS- 100 & 200 mm /min. TA-3$^{o.}$ Argon shielding gas	It is possible to make joints without the formation of martensite structure. This process improves ductility of the joints and hence FSW render the decarburization process unnecessary because it can produce ductile joints.
72	Hwang et. al. [41]	Pure copper C11000. thickness 3.1 mm	SKH9 high-speed steel, SD-12 mm PD- 3 mm	RPM- 400 to 1200. TS-20 to 60 mm/min. TA- 1^{o}	Successful welds obtained at temperatures of 460 ◦C and 530 ◦C. TMAZ attained hardness and tensile strength 60% of base materials. Three times as much elongation was attained with proper temperature control.
73	Saeid et. al. [90]	SAF 2205 duplex stainless steel. 2mm thick	WC-base tool, SD- 16 mm, PD- 5 mm PL- 1.5 mm	RPM- 600 rpm. TS- 50, 100, 150, 200, & 250 mm/min. TA-3^{o}. Argon gas shielding at a flow rate of 18 L/min	TS between 50–200 mm/min produced sound joints, but at the speed of 250 mm/min a groove-like defect was formed. Increasing TS decreased the size of alpha and gamma phases in SZ as such hardness and tensile strength increased.
74	Commin et. al. [46]	AZ31 magnesium alloy rolled sheets 2 mm thick	PD- 4-mm SD- 10mm	1000 rpm at 200mm/ min; 1300 rpm at 300 mm/min; 1400 rpm at 700	Shoulder diameter increase as well as tool rotation speed increase or welding speed decrease result in an increase in heat generated during the process and promote grain growth. Retreating side had higher stress levels.

				mm/min and 600 rpm at 2000 mm/min. F- 6.5–9 kN	
75	Barlas et. al. [91]	Pure copper sheet to brass (CuZn30). 3mm thickness	SD- 15 mm concave profile. BD- 5 mm, TD- 3mm	RPM- 800 rpm TS- 22 mm/min TA- 3º	Cu/CuZn30 joints had a tensile strength of 46% lower Cu BM and CuZn30 BM. Bend strengths were recorded to be 47% higher and 31% lower than that of Cu BM and CuZn30 BM, respectively.
76	Cui et. al. [92]	High carbon steel S70C (0.72 wt. % C). 1.6 mm thick	WC-based tool. SD- 12mm. PD-4mm. PL-1.5 mm	RPM-100–800 rpm. TS- 25-400mm/min TA-3º	Successful joining of high carbon steel without any pre- or post-heat treatment. Proper joins can be obtained by decreasing the peak temperature to below A1 and decreasing the cooling rate to less than the lower critical cooling rate. It is possible to control the cooling rate and the peak temperature in FSW unlike in fusion welding.
77	Fujii et. al. [22]	Carbon steels IF steel, S12C, S35C The plates are 1.6 mm thick	WC-based tool SD-12 mm PD-4.mm PL-1.4 mm	TS-100 – 400mm/min RPM- 400 TA- 3◦	Strength of the S12C steel joints increased with increasing welding speed, while the strength of the S35C steel joints shows a peak near 200 mm/min.

2.4 Tool Design

Colligan [21] reported that stirred material is brought to the nugget zone (NZ) by the threads when a threaded tool is used. Fujii et. al. [22] noted some tool characteristics that are necessary for effectiveness of the process. It was mentioned that an FSW tool is supposed to be both simple and produce enough mixing capabilities to obtain good joints. The effect of tool shape on mechanical properties and microstructure was studied and it was concluded that material to be joined determines the shape of the tool to be used although some materials such as AA6061-T6 are not affected by tool shape owing to their low resistance to flow. For 5083-O the tool shape required depended on the speeds used. For 1500 rpm triangular probe was the best; for 800 rpm, threaded cylindrical was the best; and for low speeds of 600 rpm, the tool shape effects were insignificant. In another research by Han [13] on AA5083-O the optimum conditions for a sound joint were found to be a traverse speed of 124 mm/min together with a rotational speed of 800 rpm using a threaded probe of 20mm diameter. Palanivel [2] investigated AA5083-H111 and AA6351-T6 revealed that straight tool profiles produced better joints while tunnel defects were observed in joints made with tapered tools. It was revealed that straight profiles have more contact area than tapered tools.

In a study carried out by Klobcar [23] on AA5083, lower hardness values were on the advancing side of the joint in relation to those observed on the retreating side. This was attributed to the high heat generation in the advancing side.

Tools are made up of a shoulder and a probe which can be integral with the shoulder or as a separate insert which could be of a different material. The shoulder and the probe design are very important aspects which determine the quality of the weld. Heat generation and the stirring action are provided by the probe.

The tool geometry plays a critical role in material flow and in turn governs the traverse rate at which FSW can be conducted [11]. The friction between the shoulder and workpiece results in the biggest component of heating. From the heating aspect, the relative size of pin and shoulder is important, and the other design features are considered not critical [11]. From the investigation done in the FS welds of very thin plates of the AA 6016-T4 aluminium alloy, it was noticed that the differences in tool geometry and welding parameters induced significant changes in the material flow path during welding as well as in the microstructure in the weld nugget [93].

Generally it has been reported that a concave shoulder and threaded cylindrical pins are used [11]. The probe is slightly shorter than the thickness of the workpiece and its diameter is typically equal to the workpiece thickness [7].

According to Venkateswarlu et. al. (2013) [47], pin diameter was found to have maximum influence among the control factors that determine tensile strength of the weld. It was outlined that the effect of shoulder diameter is not significant compared to pin diameter for weld tensile properties.

Although weld properties, defects and the forces on the tool are affected by tool design, tools are currently designed empirically by trial and error and thus work on the systematic design of tools using scientific principles are just beginning [94].

2.5 Commonly Used Tool Materials

Rai et. al. (2011) [94] suggested the tool materials that can be applied during friction stir welding. These materials include tool steel for joining aluminium and magnesium alloys; Polycrystalline cubic boron nitride (pcBN) tools for hard steel and titanium; tungsten based tools for steel and titanium alloys as well.

From the literature reviewed above, it has been shown that H13 tool steel, Die/Tool steels and Tungsten Carbide tools are commonly used in FSW of different material types. Straight tool profiles have always yielded best results as outlined by Palanivel et. al. (2012) [2]. Palanivel and Koshy (2012) [50] also carried out tests using HCHCr steel tool. Five different tool pin profiles, (SS), (TS), (SH), (SO) and (TO) were identified. Of all the tools, the straight square pin profile yielded the best results at a speed of 63mm/min in joining 6351 and 5083 AA. In another research friction stir welding tool pins like straight cylindrical, cylindrical taper, threaded cylindrical, square, and triangular with combinations of 15, 18, and 21mm shoulders were used by Elangovan and Balasubramanian to join 6061 aluminium alloy. In their investigation, square pins provided superior tensile properties with least number of defects [47].

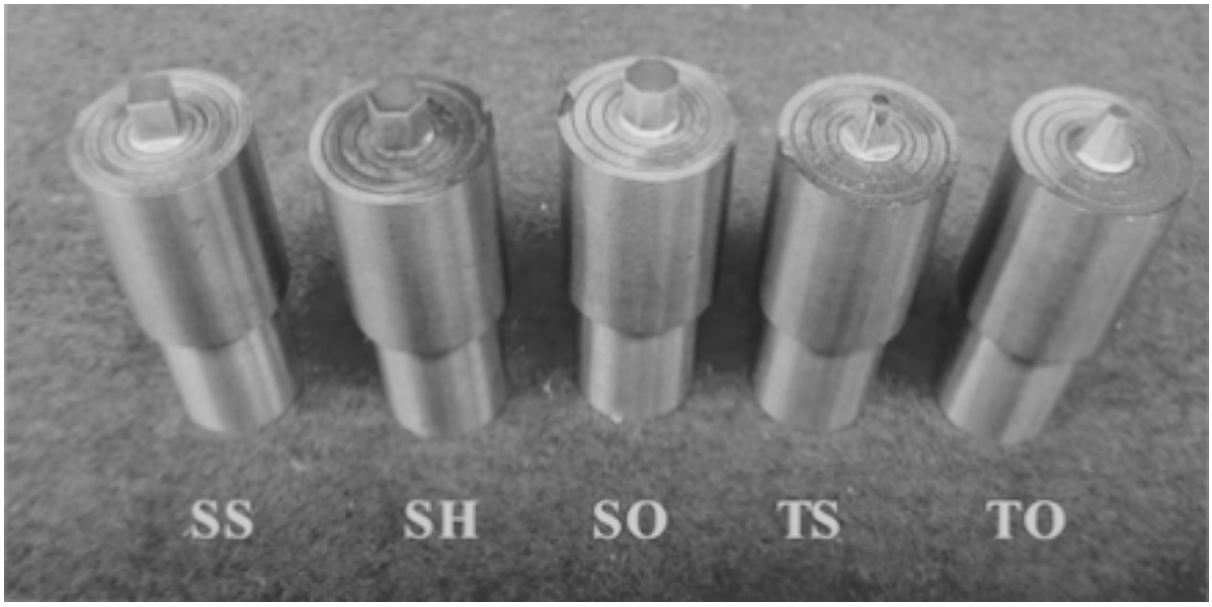

Figure 2. Tool Pin Profiles [2].

2.6 Process Parameters

According to Lee et. al. (2003) [26] and Bisadi et. al. (2012) [95], many parameters can influence the FSW joint quality and these include tool shape and geometry, tool tilt angle, rotational and welding speeds of the tool and also the load applied between the tool shoulder and the surface of the work piece especially for adjusting the welding temperature and sufficiently stirring up the sheets interface. Rodrigues et. al. (2009) [93], in the FSW of AA6016-T4 aluminium alloy, discovered that the differences in tool geometry and welding parameters induced significant changes in the material flow path during welding as well as in the microstructure in the weld nugget. Nandan et. al., (2008) [96] claimed that, the heat generation rate, temperature field, cooling rate, downward force, torque and the power depend on these variables. Torque decreases as tool rotation speed increases due to increased heat generation. It was also noticed that welding speed does not significantly affect the changes in torque. The relative velocity between the tool and the material is affected by rotational speed and hence welding speed does not affect heat generation. Heat input and temperatures are reduced by high traverse speeds because lower temperatures reduce material flow. Tool erosion or in some cases breakage may occur if there is excessive x-direction force [96]. According to Palanivel and Koshy (2012) [50], the increase in welding speed leads to an increase in the tensile strength up to a maximum value, while if we apply a further increase in the welding speed, it results in a decrease of the tensile strength of the FSW joints.

Traverse speed and rotational speed are factors that need to be taken into consideration when selecting welding parameters [17]. Fujii et. al. [22] proposed that for hard materials like 5083, the rotation speed should be decreased to attain a good weld. It was mentioned that the deformation resistance of 5083 at high temperature is greater than that of 1050 and 6061. Heidarzadeh [24] studied AA6061-T4 joints and found that the UTS increased with increasing traverse and rotational speeds as well as axial force up to a certain point after which it starts to decrease. Increasing the traverse speed increases the tensile strength whilst increasing the rotational speeds reduces the tensile strength [4, 24]. More heat can be generated by increasing rotational speed and reducing traverse speed [4, 50] which in turn increases the elongation [4]. Dinaharan [25] studied AA6061 and found that the material placed on the advancing side of the tool occupied a major part of the weld zone when tool rotational speed was increased. Four zones were found to exist and these were base metal, heat affected zone, thermo-mechanically affected zone and nugget zone. On the other hand other researchers [17, 26] studied dissimilar A356 and AA6061 and observed that the material on the retreating side prevailed more on the microstructure of the stir zone.

In a research during the welding of brass plate, it was discovered that if proper welding parameters are used, the mechanical properties of obtained weld joints can reach to base metal strength level [6].

Table 6. Main process parameters and their effect in friction stir welding.

Parameter	**Effects**
Rotation speed	Frictional heat, oxide layer breaking and mixing of material
Tilting angle	The appearance of the weld
Welding speed	Appearance, heat control
Down force	Frictional heat, maintaining contact conditions

In another study [7], in the friction stir welding of 2024 Al alloy plate to 7075 Al alloy plate, the rise in welding speed resulted in the formation of kissing bond and pores especially when the 2024 Al alloy plate was located on the retreating side. Esther and Stephen Akinlabi, (2012) [43] noted that the feed rate directly affects the quality of weld produced in the study of 5754 aluminium alloy and C11000 copper. They observed that good material mixing was achieved in welds produced at lower feed rate due to high heat generated while the welds produced at high feed rates resulted in worm hole defect formation.

The competing FSW demands led to the concept of a "processing window". This is the range of processing parameters i.e. tool rotation and traverse speed that will produce a good quality weld. Within this window the resulting weld will have a sufficiently high heat input to ensure adequate material plasticity but not so high that the weld properties are excessively deteriorated. According to Cavaliere et. al. (2006) [7], the welding speed of 2.67 mm/s is optimum, according to optimised welding parameters determined so far in the welding of 2xxx and 7xxx Al alloys.

A suitable tilt of the spindle towards trailing direction would make sure that the shoulder of the tool holds the stirred material by threaded pin and move material efficiently from the front to the back of the pin [11]. Studies have revealed that preheating or cooling may also be employed for some specific FSW processes [11]. For materials with high melting point such as steel and titanium or high conductivity such as copper, the heat produced by friction and stirring may be not sufficient to soften and plasticize the material around the rotating tool. Therefore, it will be difficult to produce continuous defect-free weld. In these cases, preheating or additional external heating source can help the material flow and increase the process window.

2.7 Microstructure

The microstructure of the joint area of AA5083 appears to be dominated by recrystallization caused by the thermal excursion of the unstable base material resulting in a zone of equiaxed grains around the weld line with more than 30 mm wide area. If the traverse speed is increased thus reducing the heat input, this would narrow this weld zone [37]. According to Moreira et. al., (2008) [16] the retreating side of 6061 macrostructure, reveals more flash and this is also the location of the lower values of hardness. FSW originates changes of microstructure. The nugget zone tend to experience high strain and is therefore prone to recrystallization. The microstructures, of base material aluminium 5083 and 6061 alloys has approximately equiaxed grains and relatively uniform grain sizes of 36 and 18 µm for the AA 5083 and AA6061 alloys respectively [97].

2.8 Microstructural Evolution

Temperature profile and history of FSW process are shown by the distinct regions at the joint. These regions are characterized by discrete microstructure sizes, shapes and varying properties, produced by the significant thermal effect and mechanical deformation. Under the heat generation, lump effect and heat transfer of the process, thermal profiles are being

distributed from the crown shaped heat source around the rotating tool to work material interface towards the outer part of work materials surfaces and edges [66]. These regions are known as weld nugget (NZ), Thermo-Mechanically Affected Zone (TMAZ), Heat Affected Zone (HAZ) and the base metal (BM).

1. The *stir zone* (NZ) is a region of heavily deformed material which symbolises the location of the tool pin during the welding process. Roughly equiaxed grains are found in this zone. It is characterised by the onion ring structure.
2. The TMAZ occurs on either side of the NZ. Strain and temperature are lower in this zone. Microstructure is more or less the same as the BM except for being partly affected by the temperature and slight deformation.
3. The HAZ is found in all welding processes. Though not deformed, this zone is subjected to a thermal cycle. Temperatures are obviously lower than TMAZ but their effect should not be overlooked.

The microstructure evolution and the resulting mechanical properties are based on the variation of the processing parameters thus creating a wide range of possible performances [57]. FSW is a solid-state process as such solidification structure is not found in the weld and the problem related to the occurrence of brittle inter-dendritic and eutectic phases is removed [7].

2.9 Hardness

Some researches were contacted by Rao et. al. (2013) [28] on Al 5083 which is a non-heat-treatable Al–Mg alloy. It was noticed that during the welding process, the high strain rate deformation and high temperatures can cause substantial microstructural variations that affect the hardness profile of the material. The weld had an average hardness of approximately 85 HV. In another study in which AA5083 and AA6061 have been joined, [3] it was recorded that at the 5083-5083 joining zone, the hardness was slightly higher than the original value because of grain refinement. However, in the 6061-6061 joining zone, the hardness dropped sharply.

2.10 Tensile Strength

Table 8 shows the results of tensile tests carried out by Shigematsu et. al. (2003) [3]. The strength of the 5083-5083 joint was 97% of that of the original material. In contrast, the strength of the 6061-6061 joint was 63% of that of the original material. The strength of the 5083-6061

joint was almost equal to that of the 6061-6061 joint. They concluded that these results show that the tensile strength of the joint is affected by the type of joint i.e. similar or dissimilar.

Table 7. Tensile strength and elongation of mother material and joint specimens [3].

	Strength (MPa)	**Elongation (%)**
Alloy		
5083	328±2	24±1
6061	320±2	16±1
Joint		
5083 - 5083	318±2	21±3
6061 - 6061	199±6	11±1
6061 - 5083	202±3	7±1

According to studies done by Esmaeili et. al. (2011) [66] using FSW of aluminium 1050/brass (70%Cu–30%Zn) of thickness 3mm, it was observed that, in any way the results of tensile tests revealed that at an optimum point, ultimate strength of the joint will reach 80% of the aluminium tensile strength. By increasing the speed of rotation, tensile strength is, however, decreased. The amount of this strength deterioration, however, depends on severity of rotation speed increase.

Parida et. al., (2012) [51], in a research in which commercial grade Al-alloy 6mm thick was FSWed, it was observed that, the tensile testing results revealed that when a comparison to base metal was made, the tensile property of the weld improved considerably and also the displacement before failure for welded plate was found to be 13 mm as compared to 7.5 mm in case of base material which indicates the increase in ductility.

2.11 Research Gap

Through assessing the researches that have been conducted in FSW, it has been established that little research work has been done on mechanical characterisation of dissimilar FSW of AA5083-H32 and AA6061-T6 aluminium alloys. As such, the mechanical properties, macro- and microstructure of these two materials when joined are not sufficiently known.

2.12 Objectives

- The aim of this research is to perform FSW welding on Dissimilar aluminum alloys AA6061-T6 and AA5083-H32 and perform analysis on:
  (i) Mechanical properties (tensile strength, microhardness).
  (ii) Metallographic properties (grain structure, grain size).
  (iii)Fractography.
- Perform regression analysis to establish the relationships between the welding parameters.

Chapter 3

RESEARCH METHODOLOGY

In this study AA6061-T6 and AA5083-H32 with dimensions 220mm x 75mm x 6mm were used. Their tensile strength values were 310 MPa and 324 MPa for AA6061-T6 and AA5083-H32 respectively. Vickers hardness values were 100 HV and 95 HV for AA6061-T6 and AA5083-H32 respectively. The chemical composition and the physical properties of these materials are presented in Table 8 and 9.

Table 8. Chemical Composition of 5083-H32 and 6061-T6.

Element	5083 (%)	6061 (%)
Magnesium (Mg)	4.00 - 4.90	0.80 - 1.18
Manganese (Mn)	0.40 - 1.00	0.0 - 0.15
Silicon (Si)	0.0 - 0.40	0.40 - 0.80
Iron (Fe)	0.0 - 0.40	0.0 - 0.70
Chromium (Cr)	0.05 - 0.25	0.04 - 0.33
Zinc (Zn)	0.0 - 0.25	0.0 - 0.23
Titanium (Ti)	0.0 - 0.15	0.0 - 0.13
Copper (Cu)	0.0 - 0.10	0.15 - 0.40
Aluminum (Al)	Balance	Balance

Table 9. Physical Properties of AA083-H32 and AA6061-T6.

Property	5083-H32	6061-T6
Density	2.65 g/cm132	2.70 g/cm³
Melting Point	570 °C	650 °C
Thermal Expansion	25 x10-6 /K	23.4 x10-6 /K
Modulus of Elasticity	72 GPa	70 GPa
Thermal Conductivity	121 W/m.K	166 W/m.K
Electrical Resistivity	0.058 x10-6 Ω .m	0.040 x10-6 Ω .m

H32 in AA5083-H32 implies that the alloy is work hardened by rolling then stabilised by low temperature heat treatment to quarter hard. AA6061-T6 implies that the alloy is solution heat treated and artificially aged. Characterisation was done by means of tensile tests, micro-hardness tests and microstructure evaluation.

3.1 Central Composite design and Response Surface Methodology

Full factorial face centred central composite experimental design was used. This was used to reduce the number of experiments required. Design Expert Software was used to generate the necessary data required for different parameter combinations as shown in Table 10. Response surfaces were also generated. The interdependence of parameters was evaluated and regression analysis was performed.

FSW welding of samples was performed using different combinations of spindle speeds and welding speeds. A total of 20 experiments were performed. Three different pin to shoulder diameter ratios, three spindle speeds and three traverse speeds were used as shown in the experimental design matrix (Table 11).

Table 10. Process parameters to be used in experiments.

Tool Ratio	**Rotational speed (rpm)**	**Welding speed (m/s)**
2.5	630	16
3.0	1000	25
3.6	1600	40

Table 11. Experimental Design Matrix.

Exp. No.	Coded Values			Actual Values		
	RPM	mm/min	Ratio	RPM	mm/min	Ratio
1	-1	-1	-1	630	16	2.5
2	1	0	0	1600	25	3
3	-1	1	-1	630	40	2.5
4	-1	1	1	630	40	3.5
5	0	0	1	1000	25	3.5
6	0	0	0	1000	25	3
7	-1	0	0	630	25	3
8	1	-1	1	1600	16	3.5
9	-1	-1	1	630	16	3.5
10	0	0	0	1000	25	3
11	0	0	0	1000	25	3
12	0	0	-1	1000	25	2.5
13	0	0	0	1000	25	3
14	0	0	0	1000	25	3
15	1	1	-1	1600	40	2.5
16	0	-1	0	1000	16	3
17	1	-1	-1	1600	16	2.5
18	0	1	0	1000	40	3
19	1	1	1	1600	40	3.5
20	0	0	0	1000	25	3

3.2 Tensile Tests

The American Society for Testing and Materials (E8/E 8M-08) guidelines were followed in preparing the tensile tests specimens. Tensile test specimen were cut in a direction perpendicular to the welding direction using wire EDM machine. The dimensions used for the tensile specimen are as shown in Fig 3 and 4. Tensile tests were done using an Instron 50 kN computerized testing machine using a cross-head speed of 1.5×10^{-2} mm/s at room temperature.

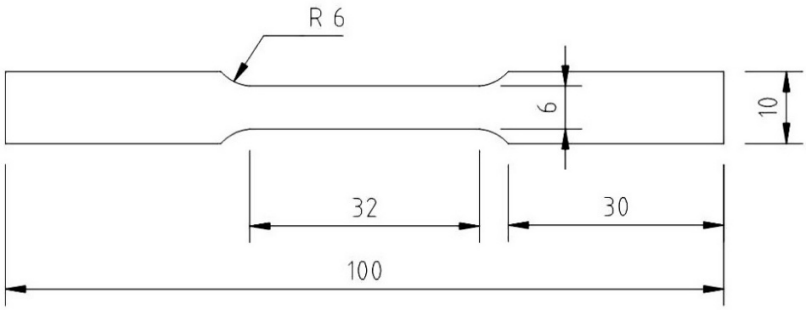

Figure 3. Tensile Test Specimen.

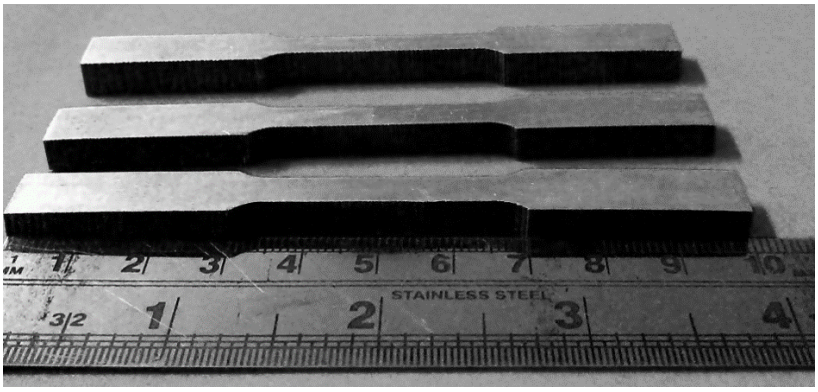

Figure 4. Tensile Test Sample Image.

Three specimen were taken from each joint and the average tensile strength was taken as the tensile strength for a particular joint.

3.3 Metallography

Metallographic examination samples were prepared by grinding and polishing until there was a mirror finish. Emery tape was used on a polishing machine in varying grades from 150, 300, 600, 800, 1000, 1200 and 1600. After this further polishing was done using alumina and diamond paste of grade 3µm and 1µm respectively. Modified Keller's reagent was used for etching. The composition of the etchant was; 2.5 ml HNO_3, 1.0 ml HCl, 1.5 ml HF, 95 ml H_2O and the etching time was 60 sec. The samples were held in Bakelite.

Vickers micro-hardness tests were carried out on a LEICA VMHT AUTO computerised machine using a 100g load and a dwell time of 10 sec. Grain structure was analysed using optical microscopy. The metallographic operations were done on a plane perpendicular to the joint main axis.

The Scanning Electron Microscopy (SEM) was used to examine the joint interface to determine joint properties; grain structure, mixing and grain size. Fractography was also done using the same machine.

3.4 FSW Tools

The FSW tools were made of AISI H13 which is a Chromium Hot Work Steel grade Tool Steel. It is composed of (in weight percentage) 0.32-0.45% Carbon (C), 0.20-0.50% Manganese (Mn), 0.80-1.20% Silicon (Si), 4.75-5.50% Chromium (Cr), 0.3% Nickel (Ni), 1.10-1.75% Molybdenum (Mo), 0.80-1.20% Vanadium (V), 0.25% Copper (Cu), 0.03% Phosphorus (P), 0.03% Sulphur (S), and the base metal Iron (Fe). Other designations of AISI H13 tool steel include UNS T20813 and AISI H13.

Table 12. Chemical composition of H13.

C	Cr	Mn	Mo	Si	V
0.32 - 0.45	4.75 - 5.50	0.20 - 0.60	1.10 - 1.75	0.80 - 1.25	0.80- 1.20

Three different threaded cylindrical tools were made. All of them had pin diameter and pin length of 6 mm and 5.8 mm respectively. They had a 1 mm pitch left hand thread. The three tools have different shoulder to pin diameter ratios which were 2.5, 3 and 3.5. As such the shoulder diameters were 15 mm, 18 mm and 21 mm for the three different type of tools used. The tool profiles used are shown in Fig. 5 and the tool configurations were made as per the dimensions shown in Table 13.

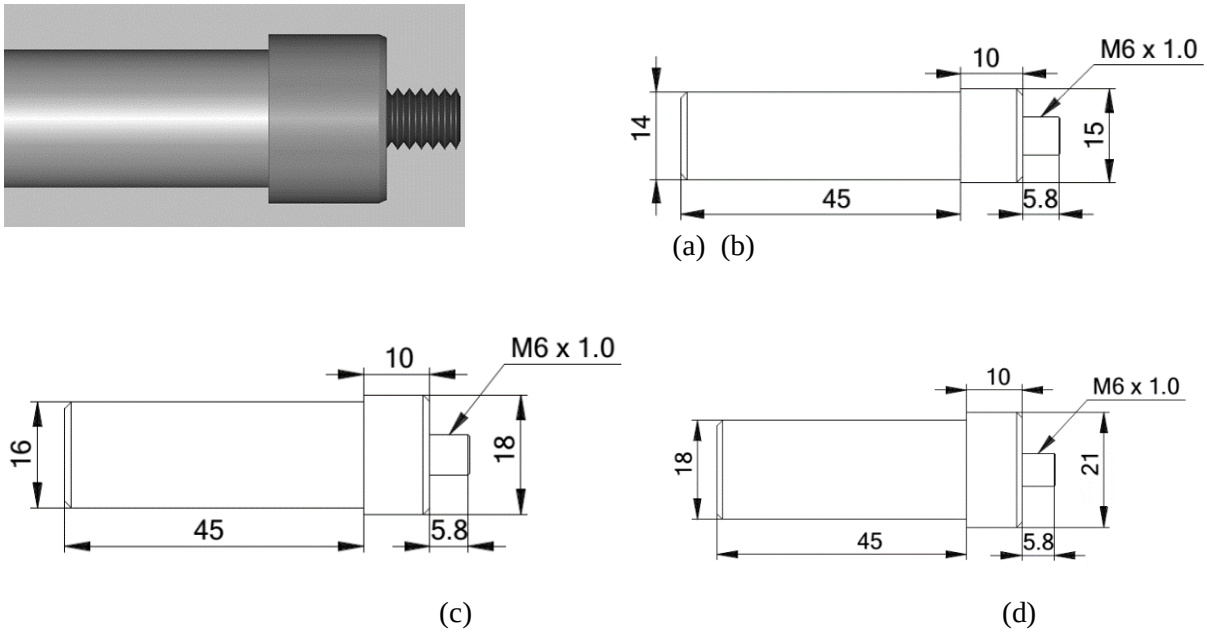

Figure 5. FSW threaded cylindrical tool profiles (a) pictorial view (b), (c) and (d) tools for pin diameter to shoulder diameter ratios 2.5, 3.0 and 3.5 respectively.

Table 13. Different dimensions for the three tool configurations used.

	Configuration 1	**Configuration 2**	**Configuration 3**
Shoulder Dia.	15 mm	18 mm	21 mm
Pin length	5.8 mm	5.8 mm	5.8 mm
Pin to Dia. Ratio	2.5	3.0	3.5

3.5 The FSW Procedure

The joining process was carried out on a 3.2kW vertical milling machine. The materials were placed on a welding fixture with a backing plate to prevent the tool to perforate through the materials and damage the machine table. The fixture allowed for the bolting and secure clamping of the materials to prevent any movement during the joining process. After the assembling, the fixture was bolted onto the machine table and the materials were ready for joining. The welding direction was parallel to the rolling direction of the aluminium plates. Threaded cylindrical tools made from H13 tool steel were used. They had pin to shoulder diameter ratios of 2.5, 3.0 and 3.5, pin diameter of 6mm with a 1mm pitch thread and a pin length of 5.8 mm. The tool rotation speeds used were 630, 1000 and 1600 rpm and traverse speeds of 16, 25 and 40 mm/min were employed. 20 dissimilar joints were made for AA5083-H32 and AA6061-T6 combination according to the parameter combinations obtained by

Central Composite Design. In all the joints AA5083-H2 was placed on the advancing side for all joints. Joints were also made on similar materials for comparison purposes.

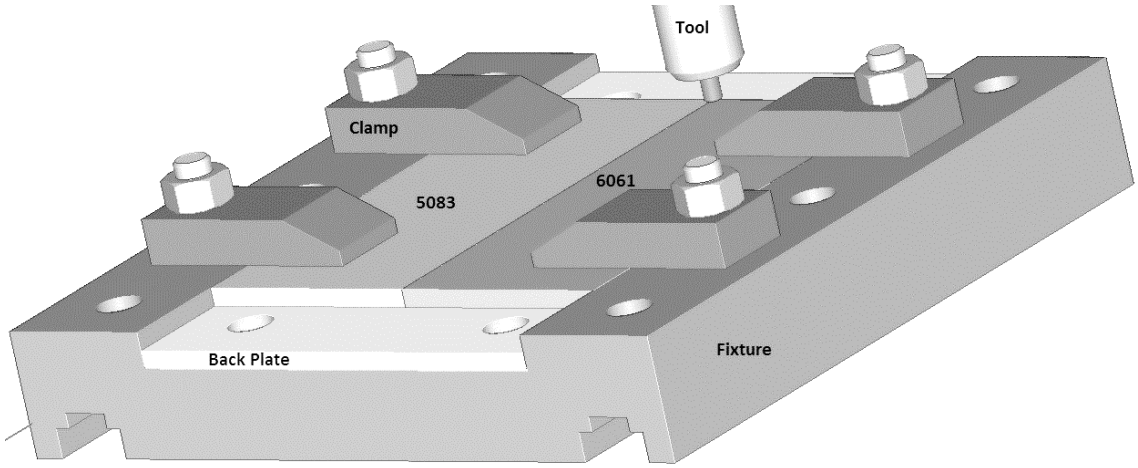

Figure 6. FSW fixture, back plate, clamps and work pieces in position.

A fixture and backing plate made of mild steel were fabricated. The fixture was used to hold the back plate and the work samples in place during the welding process. It ensured that there were no vibrations during the fabrication process as well as firmly holding the back plate and work pieces in place. The back plate was made of mild steel. The purpose of the back plate is to provide a cushion to the fixture so that it is not damaged by the tool during the joining process.

Chapter 4

RESULTS AND DISCUSSION

The dissimilar joints AA6061-T6 and AA5083-H32 were successfully joined by the Friction Stir Welding process and showed no visible defects from the outside. For each of the available parameter combinations dissimilar joints were made and 20 experiments done were successful without visible external defects. Joints were also obtained on similar materials using predetermined parameters.

4.1 Tensile Tests

The tensile strength of all the joints were lower than those of the base material, regardless of the rotational speeds and welding speeds as previously noted by Heidarzadeh [24]. Tensile tests were carried out and Table 14 gives the results of the tests.

The dissimilar joints were successfully obtained at various speeds and feeds. The strongest joint had a maximum tensile strength of 230 MPa. This strength is 74% of AA6061-T6 base material. This is attributed to the fact that AA5083-H32 material is placed on the advancing side and thus as the speed increases the material placed on the advancing side of the tool occupied a larger portion of the weld zone [25]. This is based on the analysis that AA6061-T6 had an inferior strength of 72.5%. Most failure occurred in the HAZ on the AA5083-H32 side of the joint. This is because since this alloy was placed on the advancing side of the tool more heat was generated on this side of the joint and thus the adverse effects of excessive heating were more pronounced on the AA5083-H32 side of the joint. However some joints also failed in the SZ.

Figure 7. Samples Showing the Failure Regions.

Welding strength improved with increase in rotational speed after which it later declined. The strongest joint was obtained at 1000 rpm, 40 mm/min using 3.0 pin to shoulder diameter ratio. The effect of improving strength with increasing speed was also noticed elsewhere [39].

Three Joints of AA5058-H32 were prepared using predetermined parameters which are; 1000 rpm, 40mm/min and 3.0 pin diameter to shoulder diameter ratio. These values were selected based on the trial runs that were performed which showed that optimal strength was approached when these parameters were used. The strength of AA5058-H32 joint was found to be 243MPa which is 75% of the base material. This is lower compared to 97% obtained by Shigematsu [3]. However, Shigematsu [3] used higher traverse speeds than those used in this research. The low strength value obtained for AA5083-H32 joint is attributed to high deformation resistance of AA5083-H32 at high temperatures caused by high rotational speeds [10]. This joint failed in the HAZ which also had the lowest micro-hardness value. The stress-strain graphs for the various combinations of the materials are shown in Fig. 8-11.

Table 14. Tensile test results for 5083-H32 – 6061-T6 joint.

S/N	Coded Values			Actual Values			Tensile Strength (MPa)
	RPM	mm/min	Ratio	RPM	mm/min	Ratio	
1	-1	-1	-1	630	16	2.5	180
2	1	0	0	1600	25	3	190
3	-1	1	-1	630	40	2.5	160
4	-1	1	1	630	40	3.5	165
5	0	0	1	1000	25	3.5	147
6	0	0	0	1000	25	3	145
7	-1	0	0	630	25	3	142
8	1	-1	1	1600	16	3.5	175
9	-1	-1	1	630	16	3.5	191
10	0	0	0	1000	25	3	118
11	0	0	0	1000	25	3	122
12	0	0	-1	1000	25	2.5	145
13	0	0	0	1000	25	3	115
14	0	0	0	1000	25	3	117
15	1	1	-1	1600	40	2.5	200
16	0	-1	0	1000	16	3	121
17	1	-1	-1	1600	16	2.5	180
18	0	1	0	1000	40	3	230
19	1	1	1	1600	40	3.5	215
20	0	0	0	1000	25	3	220

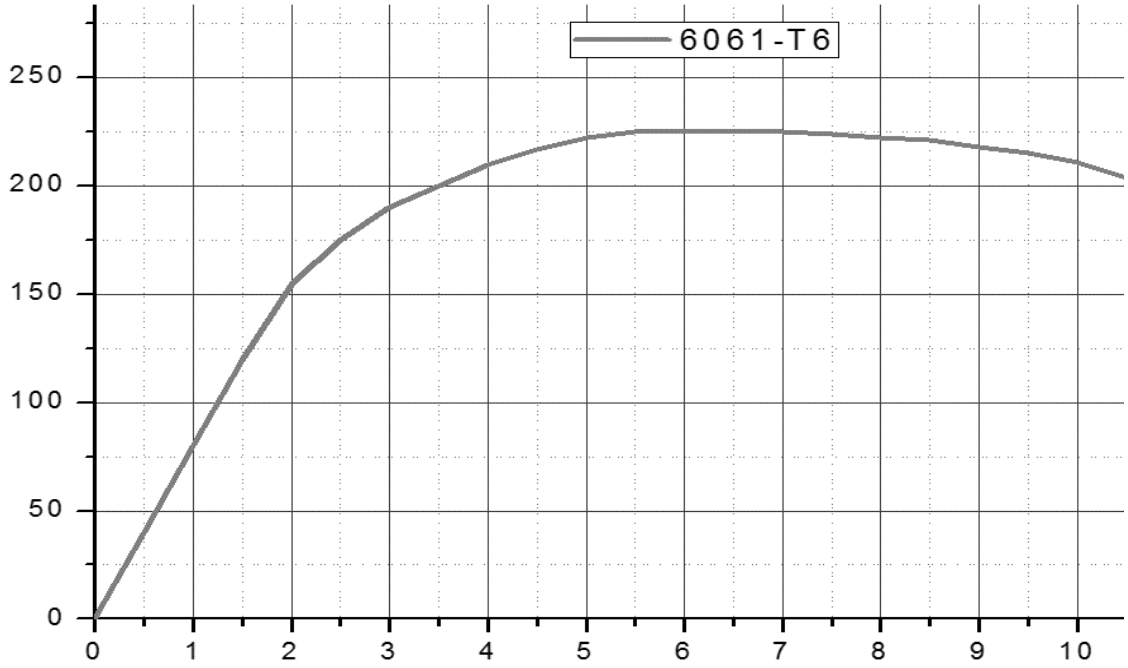

Figure 8. Stress-Strain graph for AA6061-T6.

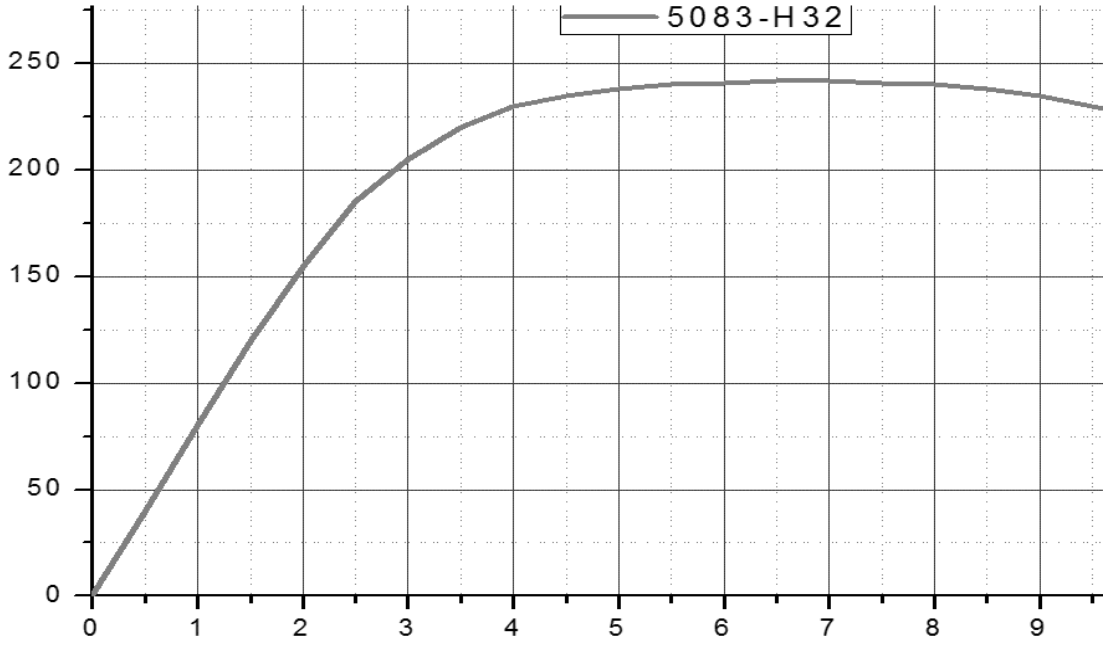

Figure 9. Stress-Strain graph for AA5083-H32.

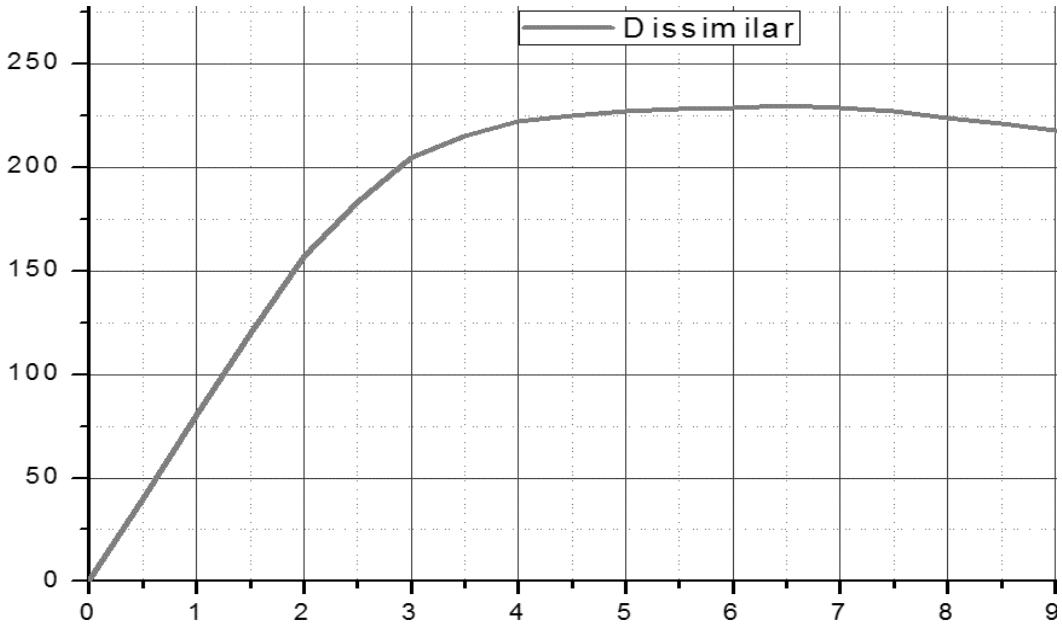

Figure 10. Stress-Strain graph for Dissimilar Joint.

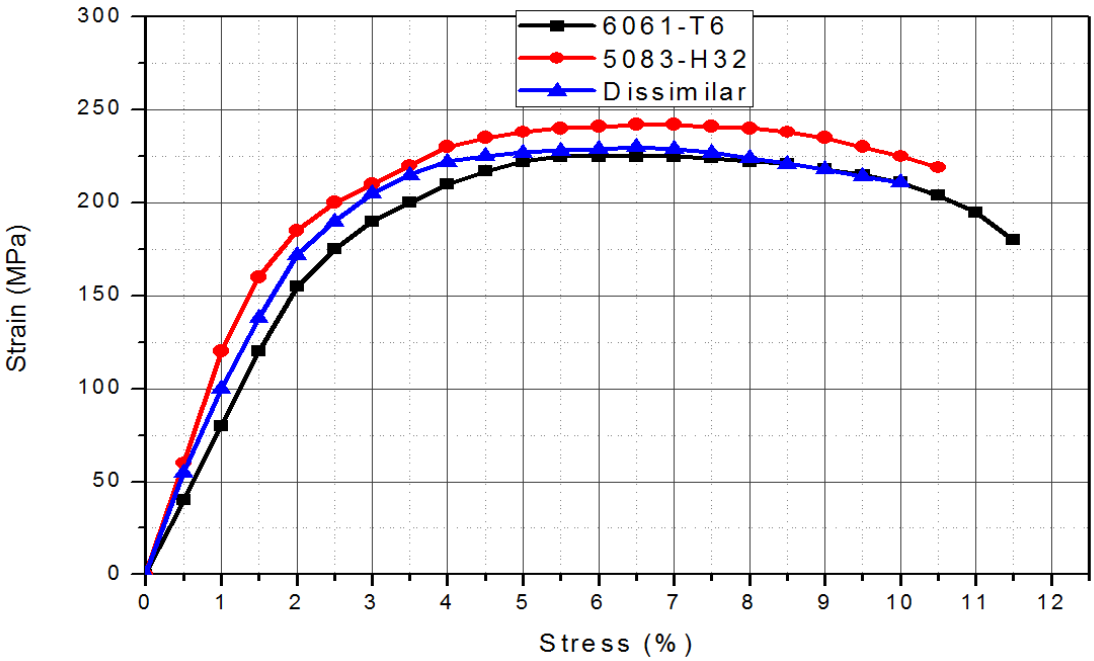

Figure 11. Combined Stress-Strain graphs for all materials.

The joint made of AA6061-T4 was prepared using the parameters 630 rpm, 25mm/min and 3.0 tool pin to shoulder diameter ratio. These values were justified as provided by the trial runs conducted which showed better welds performed using these parameters. This material gave the least mechanical strength. The resulting 225MPa which is 72.5% joint strength was in agreement to the observations made by Khorsid et. al. (Personal communication, 2012) who noticed that the joint strength of AA6061 should be expected to exist within 65% to 110% of

the base metal strength. This joint failed in the HAZ where lowest hardness values were recorded.

4.2 Macro- and Microstructure Analysis

4.2.1 Macrostructure

The weld joint had a smooth appearance but it had some visible Semi-circular features which curved towards the trailing side of the welding direction. This is attributed to the rubbing of the tool shoulder on the aluminium plates being joined [50]. There was a flash on the retreating side of each joint and similar observations were made by Moreira et. al., (2008) [16]. The distribution of the different zones i.e. Base material, Thermo-mechanically affected zone (TMAZ), Stir Zone (SZ) and Heat Affected Zone (HAZ) is as show in Fig. 12.

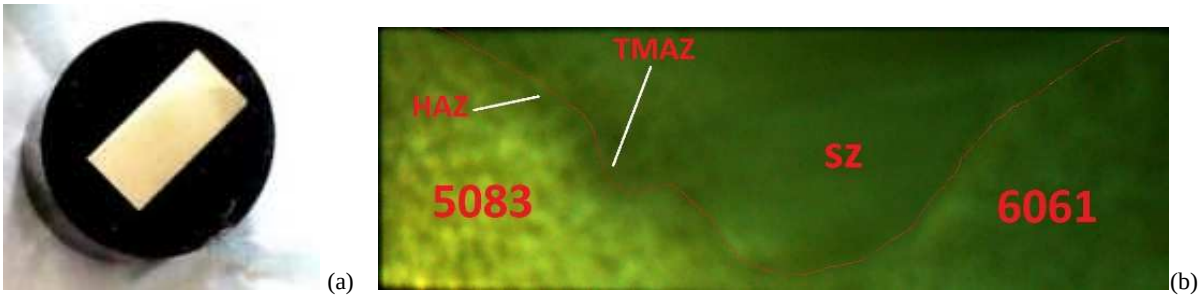

(a) (b)

Figure 12. Macrostructure of the Dissimilar Joint after Etching.

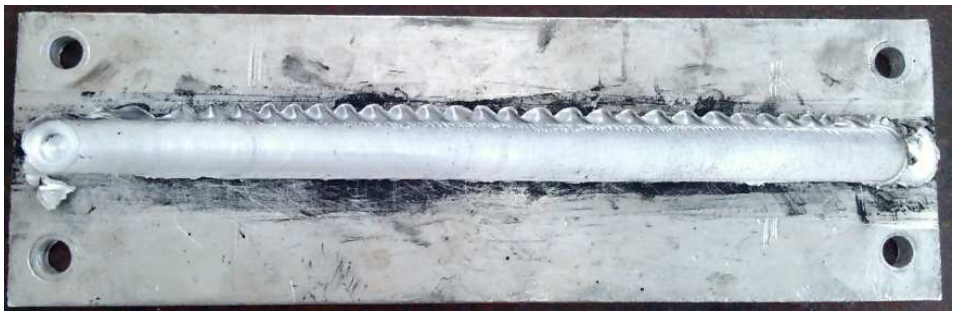

Figure 13. Flash observed on the retreating side of the joint.

4.2.2 Microstructure

Optical micrographs of the dissimilar joint as well as AA5083-H32 and AA6061-T6 alloys were taken and are presented in Fig. 14. The microstructure of the dissimilar AA5083-H32 and AA6061-T6 joint revealed fine particles within the joint. The grains were smaller compared to the base material. Such a phenomenon is attributed to recrystallization as previously noted by other researchers [23]. The alternating light and dark particles in the dissimilar joint is a manifestation of the intermixing of AA6061-T6 and AA5083-H32 particles. The lighter colour

to the right of the dissimilar joint represents AA6061-T6 alloy whilst the dark side is AA5083-H32 alloy. Some defects were noticed upon magnification by the microscope.

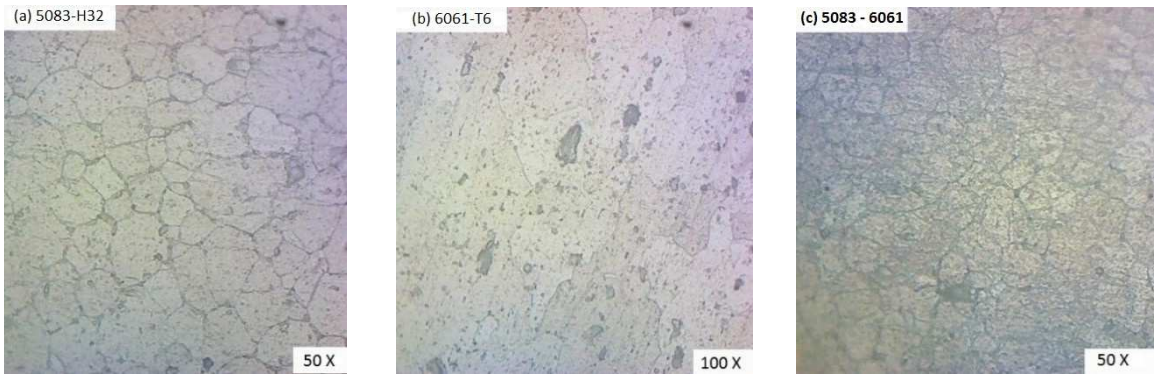

Figure 14. Microstructures of nugget zones of (a) AA5083-O (b) AA6061-T4 and (c) AA5083-H32 & AA6061-T6.

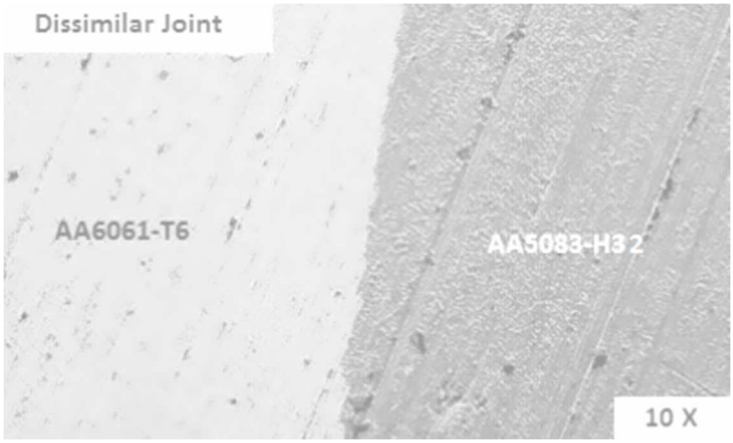

Figure 15. Dissimilar joint interface.

4.2.3 Scanning Electron Microscopy

SEM was used to give finer details of the joint. SEM Fractography on the fracture location revealed that the joint had numerous voids at micro level. This implies that the joint was porous. The porosity could be the main cause of failure. This porosity could be attributed two phenomenon; first this could be lack of enough plasticising of the materials during processing as such the joints appear to be fibrous. Second, there could have been excessive heating as well as trapped air inside the joint and porosity was therefore a result of trapped air trying to escape from an overheated material which can offer less resistance to passing air.

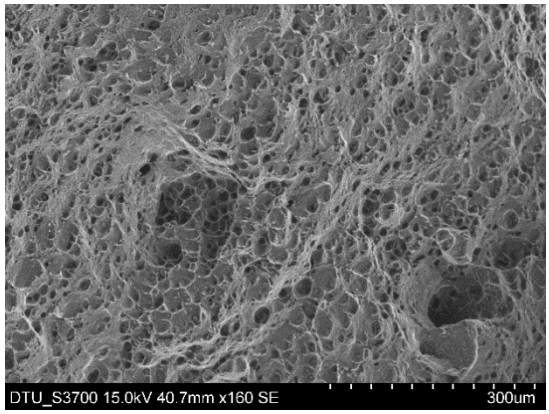

Figure 16. SEM Fractography of the joint fracture.

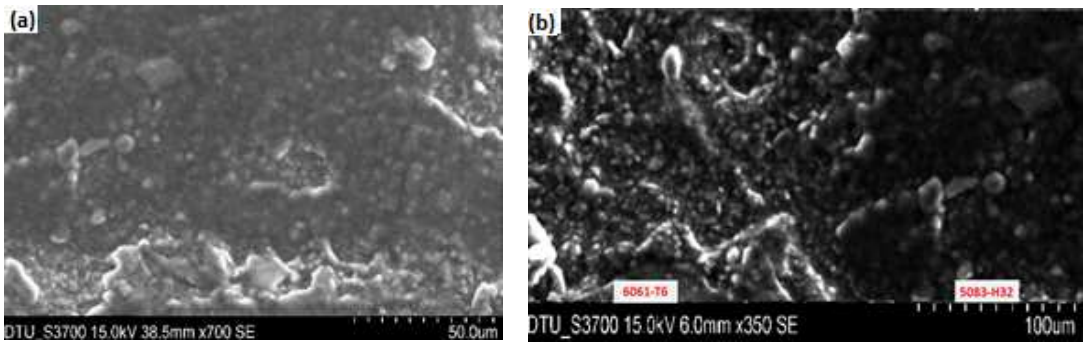

Figure 17. SEM micrograph of the cross-section of the welded joint of the dissimilar materials 5083-H32 and 6061-T6.

SEM images of the dissimilar joint revealed that the grains at SZ were very. This is the reason why the SZ was generally stronger than the TMAZ and HAZ. The fine grains are due to recrystallization. The nugget zone tend to experience high strain and is therefore prone to recrystallization.

4.3 Micro-Hardness

The hardness values of all joints were generally decreasing from the top to the bottom of the joint. At a distance of about 1200 µm just below the top surface, there was a sharp increase in microhardness values in all cases. This phenomenon could be attributed to the rapid cooling effect of the upper part of the joint due to exposure to the open air. On the other hand at about 1200 µm from the bottom there was a drop on microhardness values probably due to slower cooling compared to the top surface.

When the microhardness values were measured across the joint, the readings were plotted as a function of distance from welding centre. There was a generally increasing trend in hardness values as we moved from the advancing side to the retreating side of the joint. The low hardness

values in the advancing side of the joint are attributed to higher temperatures generated in the advancing side. Similar results were also demonstrated by Klobcar [23]. The lowest hardness values of the joints were found in the HAZ.

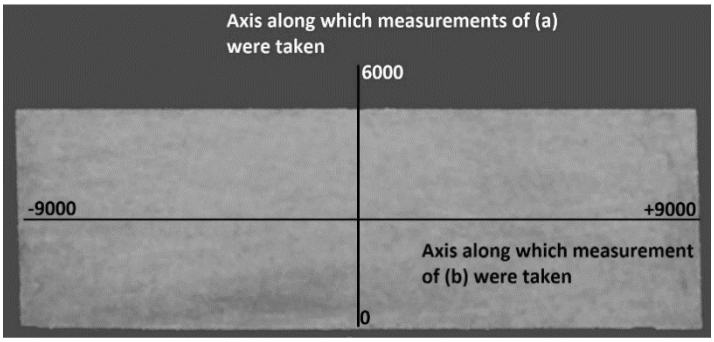

Figure 18. Work Sample Used for Microhardness Measurements.

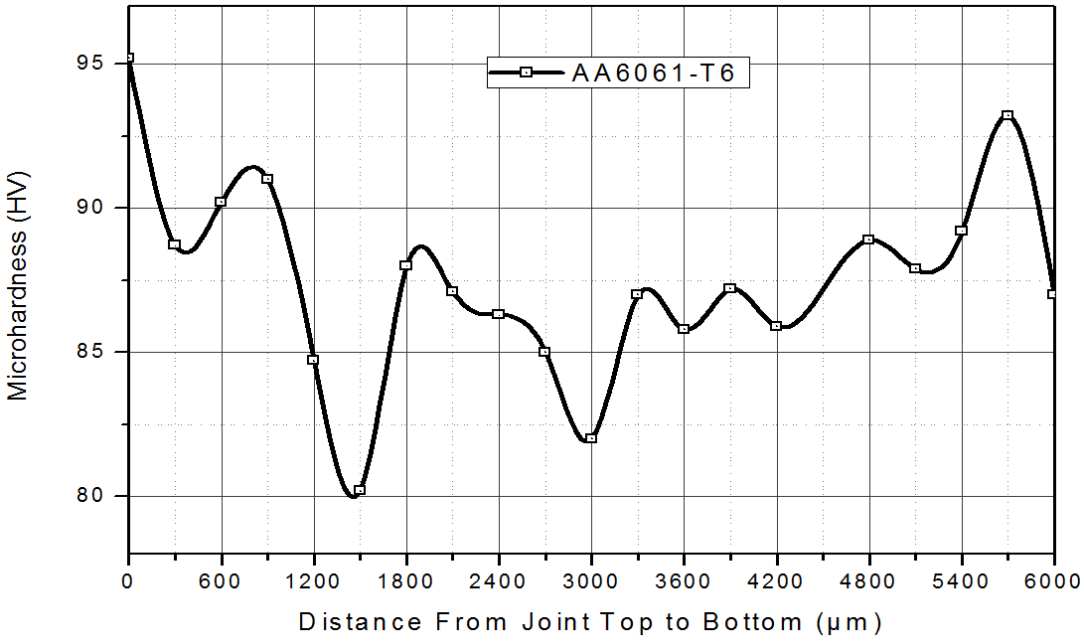

Figure 19. Hardness values of AA6061-T6 from top to bottom.

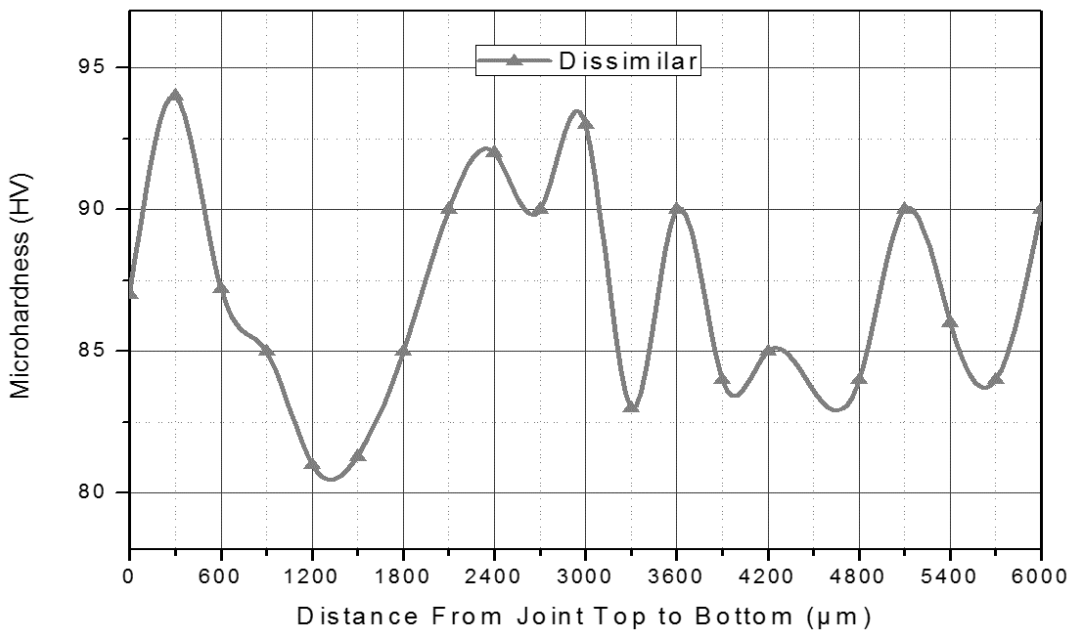

Figure 20. Hardness values of dissimilar joint from top to bottom.

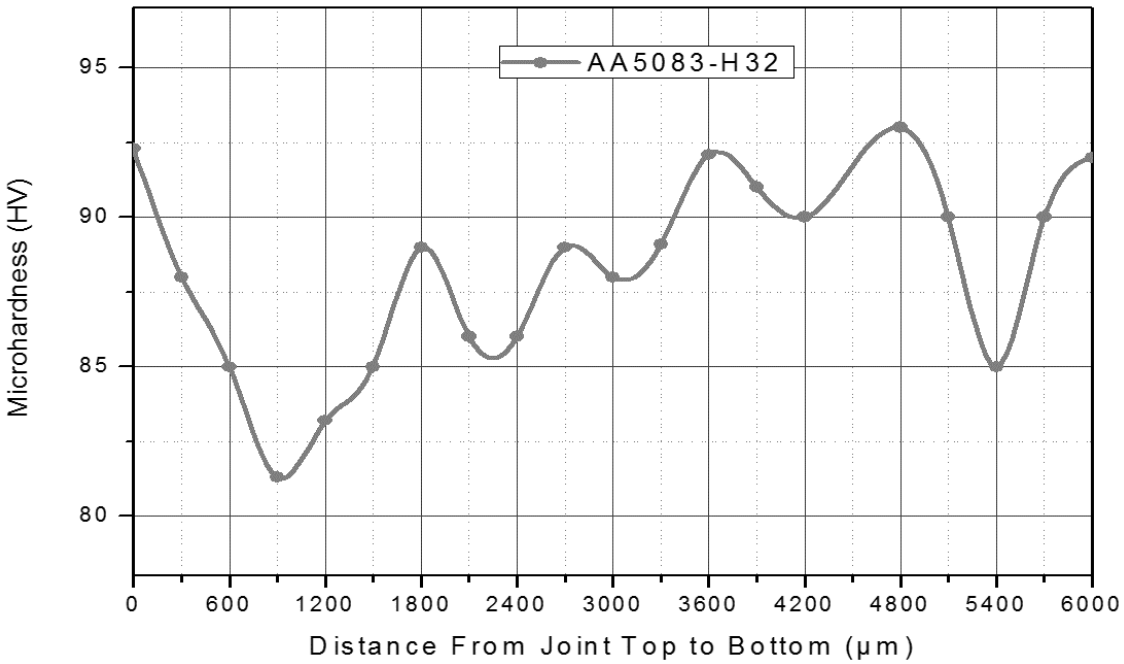

Figure 21. Hardness values of AA5083-H32 from top to bottom.

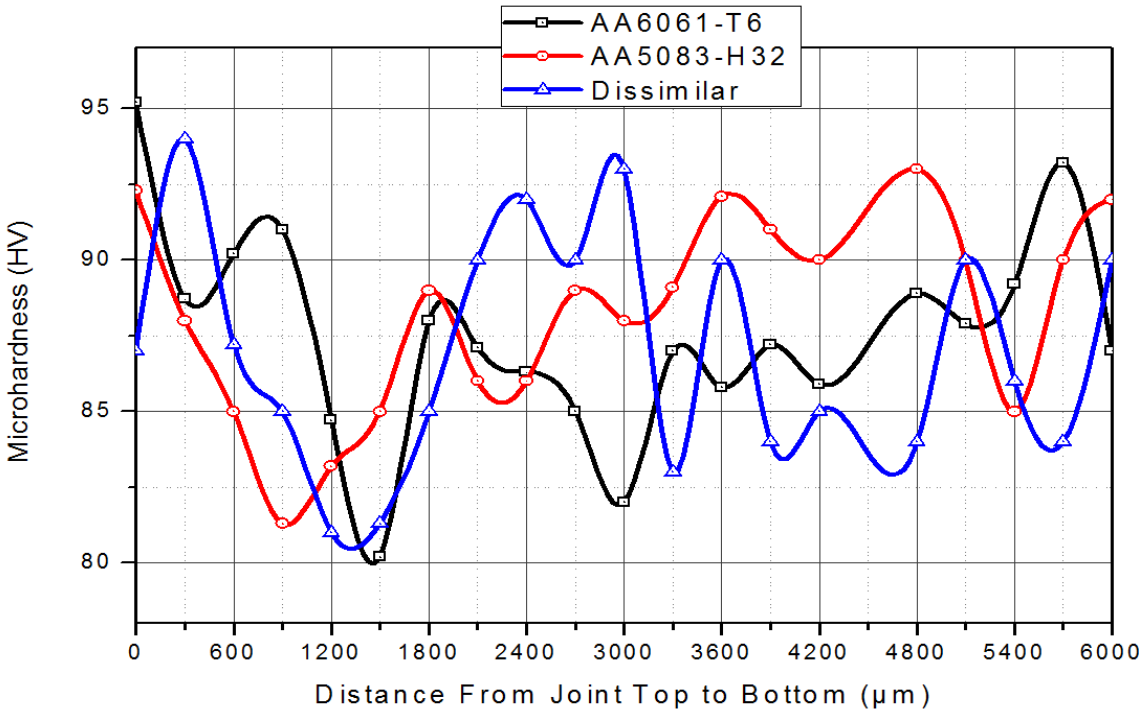

Figure 22. Hardness values of all joints from top to bottom.

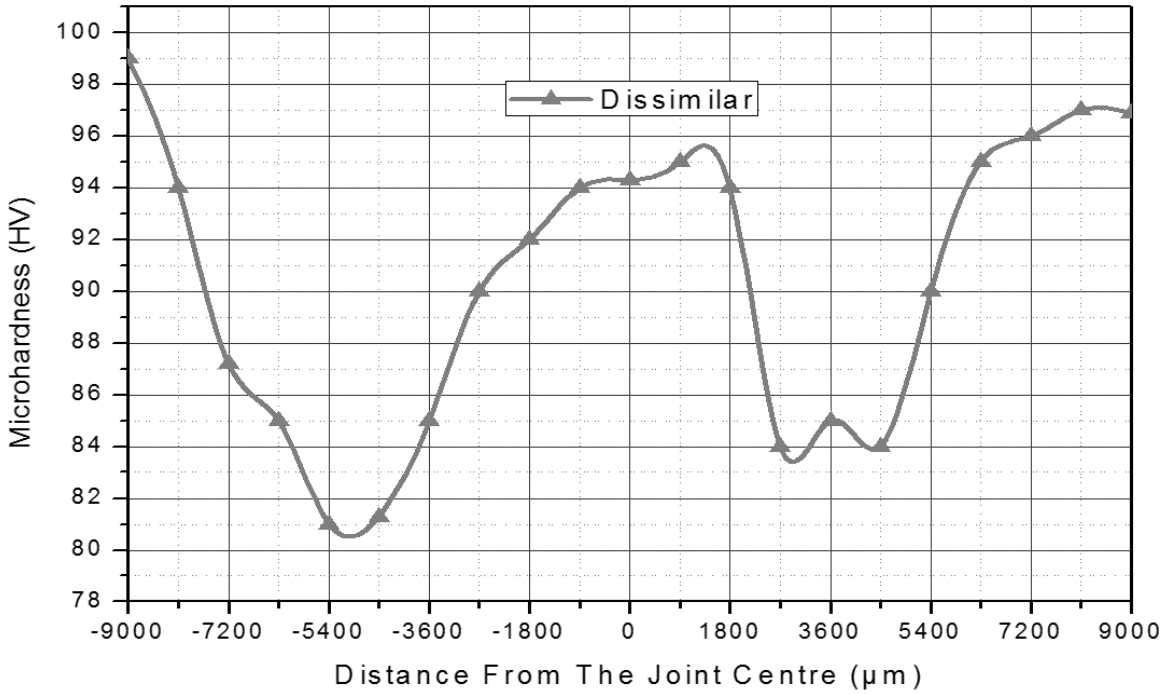

Figure 23. Hardness values of dissimilar joints from the centre towards the advancing and retreating sides.

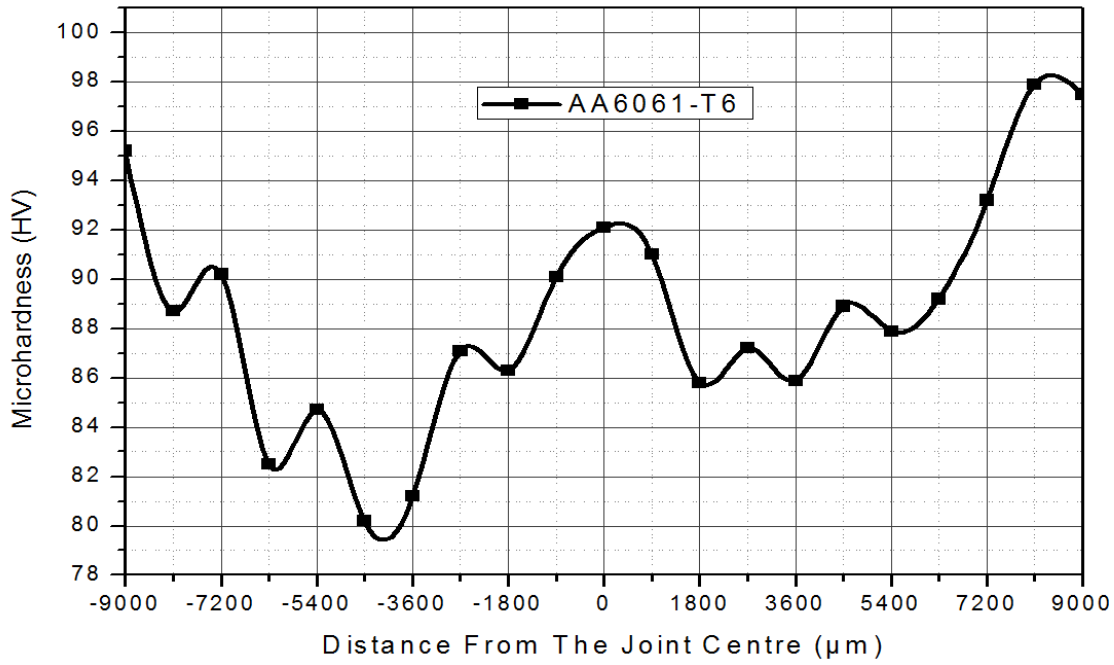

Figure 24. Hardness values of AA6061-T6 from the centre.

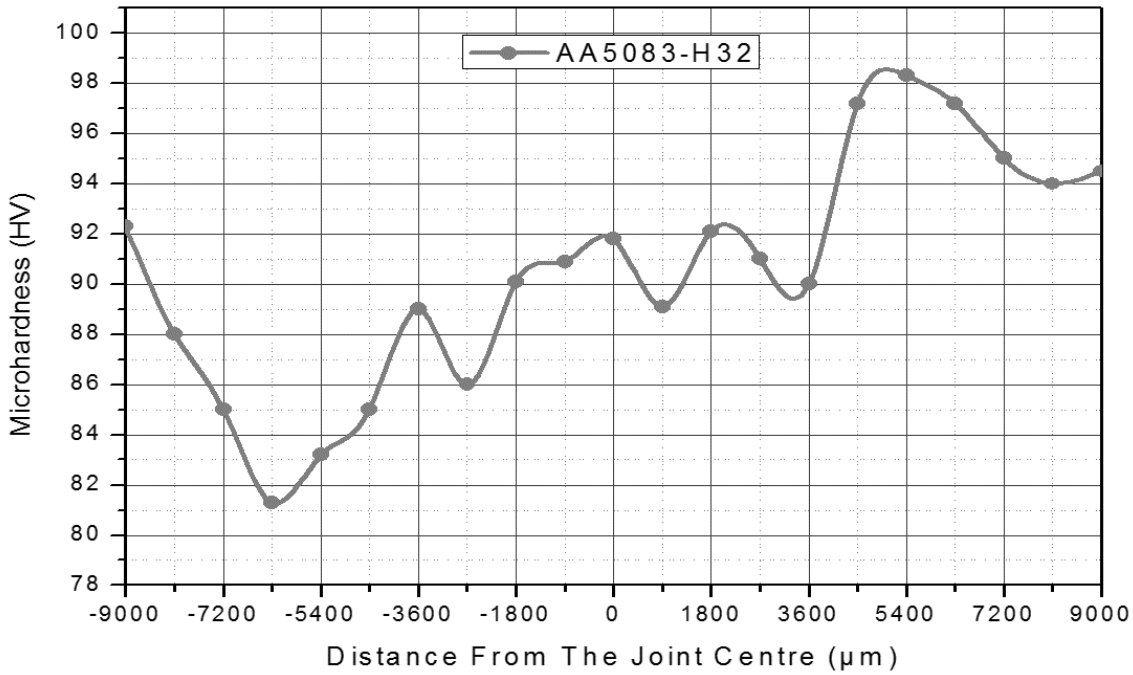

Figure 25. Hardness values of AA5083-H32 from the centre.

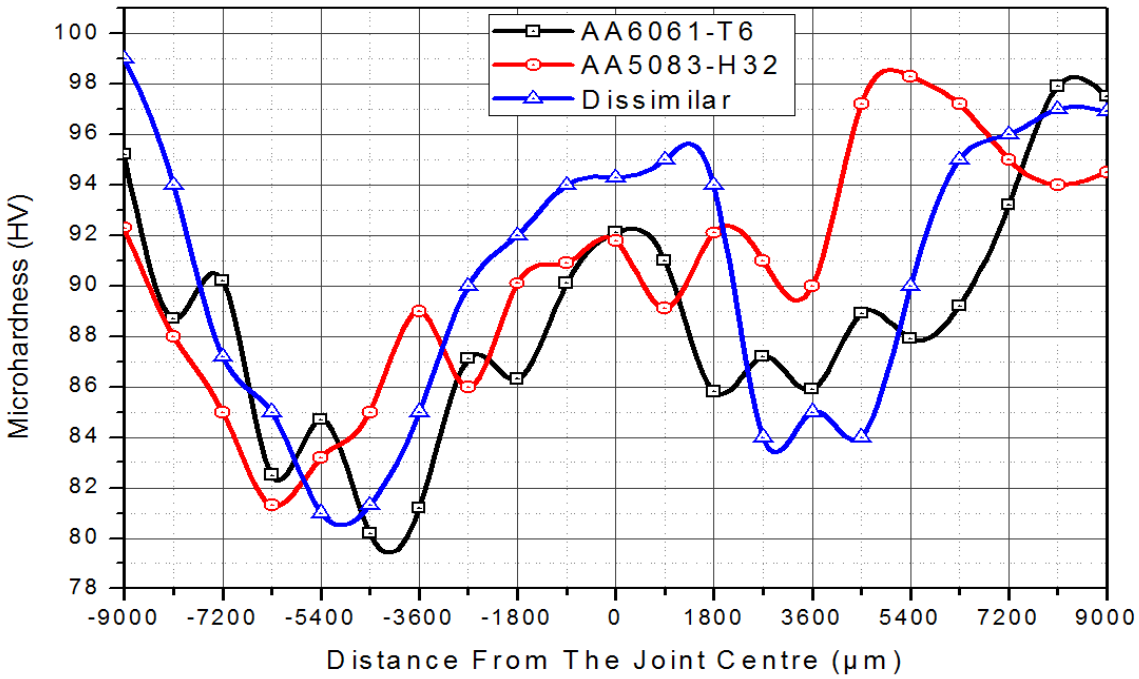

Figure 26. Hardness values of all joints from the centre.

Generally the hardness values of the nugget zone were notably lower than the base alloys. Similar observations were made by Moreira [4]. It was also observed that the temperatures on the advancing side were found to be slightly higher than those on the retreating side. The hardness at the Thermo-Mechanically Affected Zone (TMAZ) was found to be about 80% of the base metal. It was found that the change in hardness occurred more rapidly at the advancing side (AS) than at the retreating side (RS). There was a sharp decrease in hardness in the HAZ to the TMAZ at the advancing side while at the retreating side, this gradient was reported to be small. An asymmetric shape on microhardness was attained and this was also reported previously [28].

4.4 Response Surface Methodology

A quadratic regression (Equation 1.) model was developed in RSM which gave the relationships among variables to obtain a particular response (Tensile strength). This equation can be used to predict the tensile strength given any parameter input into the system. Optimisation can therefore be done based on this regression equation.

$$\sigma = 145 + 24A - 13B + 4.67C - 68.5AB + AC + 21A^2 + 98B^2 + C^2 \qquad \textit{Equation 1}$$

Where: A = Rotational speed; B = Traverse; C = Pin to shoulder diameter ratio

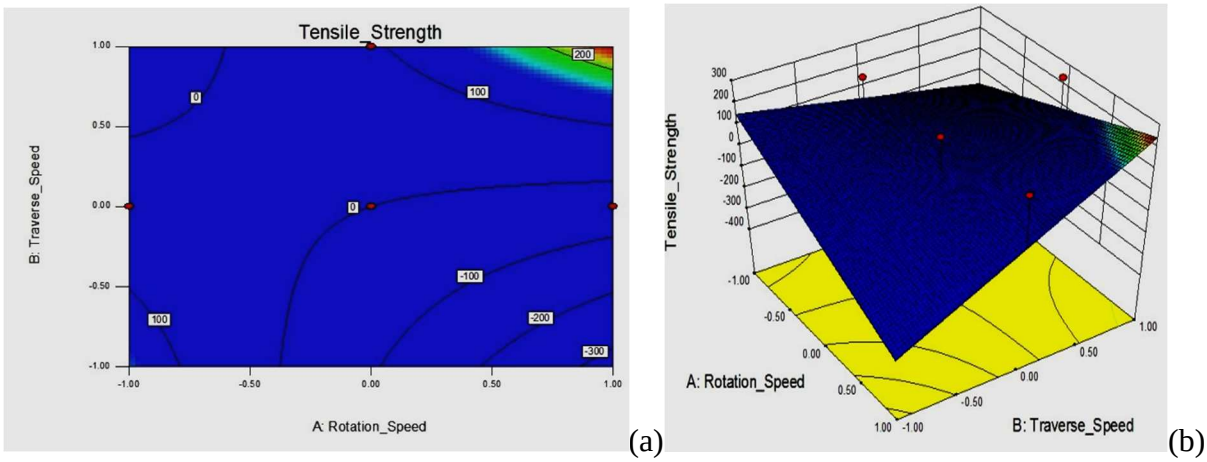

(a) (b)

Figure 27. Contour Plot (a) and Response Surface (b) for traverse and rotational speed.

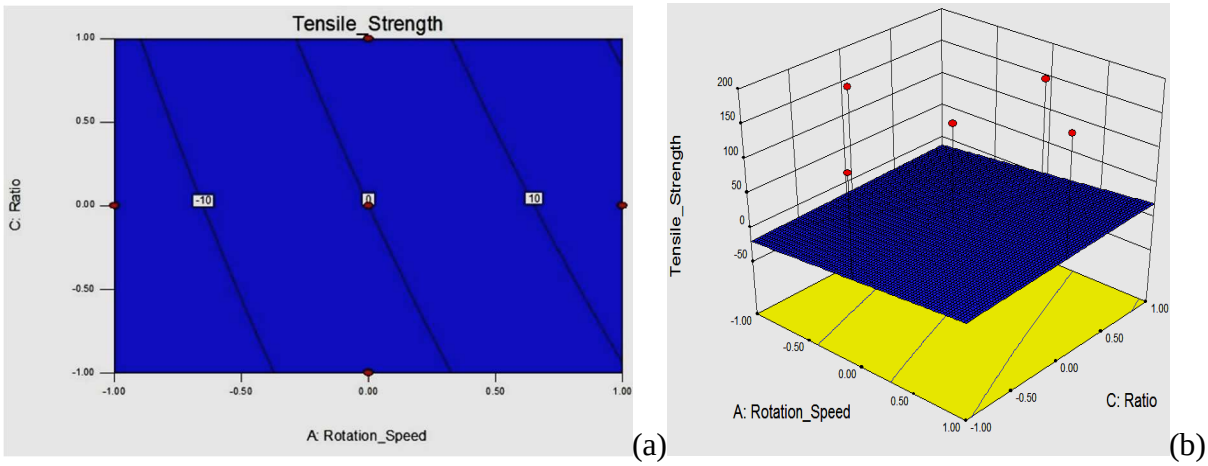

(a) (b)

Figure 28. Contour plot (a) and response surface (b) for rotation speed and ratio of pin to shoulder diameter.

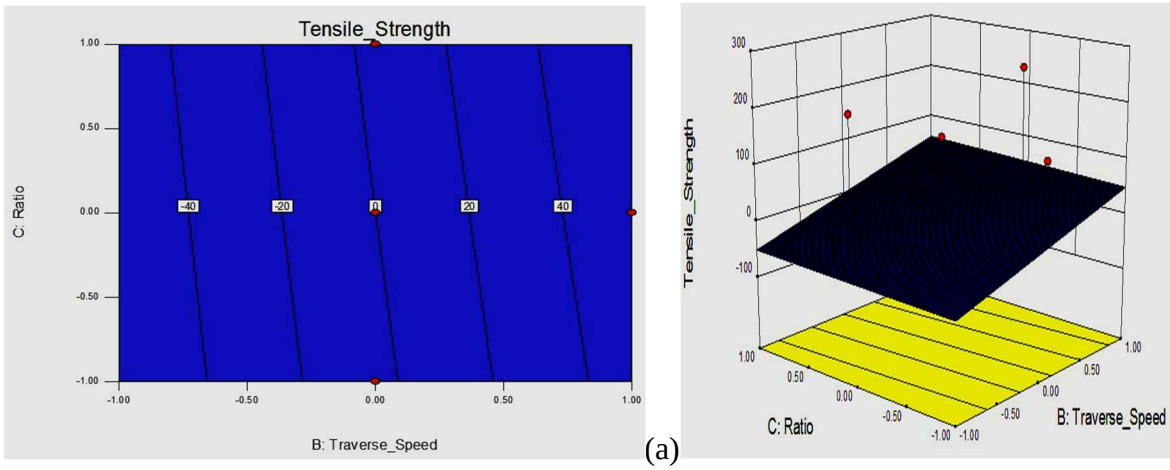

(a) (b)

Figure 29. Contour Plot (a) and Response surface (b) for traverse speed and ration of pin to shoulder diameter.

The contour plot and the response surface of the traverse and rotational speeds and pin to shoulder diameter ration used are as provided in Fig. 27 -29. It was shown (by the response surfaces) that any increase in traverse speed is supposed to be complimented by a proportional increase in rotational speed in order to maintain optimal results. The tool pin to diameter ratio has shown that it has a minimal effect to the tensile strength of the joint. Increasing the traverse speed had an effect of increasing the tensile strength. Also, it has been shown that traverse speed has more effect to the tensile strength compared to rotational speed. The regression equations giving the relationships between rotational speed, the traverse speed and pin to shoulder diameter ratio are given in Equations (2-4).

$$\sigma = -45.43A + 91.14B + 196.5AB \qquad \textit{Equation 2}$$

$$\sigma = 15.33A + 4.67C + AC \qquad \textit{Equation 3}$$

$$\sigma = 54.8B + 4.67C + BC \qquad \textit{Equation 4}$$

Chapter 5

SUMMARY AND CONCLUSIONS

In this research work, mechanical characterisation, process modelling, microstructure and fracture properties of friction stir welded AA5083-H32 and AA6061-T6 have been addressed. Spindle speed and rotational speed are the most important factors for producing sound welds. It has been noted that some materials are more readily weldable than others as witnessed by the difficulty with which AA5083-H32 was joined. Several conclusions have been made and these are outlined as follows;

1. The dissimilar joint exhibited intermediate values of tensile and microhardness properties when compared to the base materials.
2. The nugget zone tend to experience high strain and is therefore prone to recrystallization.
3. Microhardness increased from the bottom to the top of the weld due to rapid cooling at the top surface of the weld being exposed to atmospheric air. Lower hardness values were on the advancing side of the joint in relation to those observed on the retreating side. This was attributed to the high heat generation in the advancing side.
4. Hardness at the Thermo-Mechanically Affected Zone (TMAZ) were found to be about 80% of the base metal
5. The nugget zone of the dissimilar joint has smaller grain sizes compared to the base materials due to recrystallization.
6. Material placed on the advancing side dictated the performance of the joint as more material within the joint was derived from the material placed on the advancing side.
7. AA5083-H32 exhibited more resistance to deformation and thus it requires more heat to be plasticised.
8. Joint efficiencies relative to the base materials varied from 57.1% to 77.7% and Joint failures were recorded in regions of lowest hardness values.
9. Change in hardness occurred more rapidly at the advancing side (AS) than at the retreating side (RS) and There was a sharp decrease in hardness from the HAZ to the TMAZ at the advancing side while at the retreating side was small. An asymmetric shape on hardness profile was attained.
10. In general, the welding strength improves with increased tool rotation speed as well as traverse speeds but traverse speed has more effect to the tensile strength compared to rotational speed.

11. SEM image on the fracture location revealed numerous voids at nano level implying that the joint was porous. The porosity could be the main cause of failure. This porosity was attributed two phenomenon; first this could be lack of enough plasticising of the materials during processing as such the joints appear to be fibrous. Second, there could have been excessive heating as well as trapped air inside the joint and porosity was therefore a result of trapped air trying to escape from an overheated material which can offer less resistance to passing air.
12. It was shown (by the response surfaces) that any increase in traverse speed is supposed to be complimented by a proportional increase in rotational speed in order to maintain optimal results.
13. The tool pin to diameter ratio has minimal effect to the tensile strength of the joint.

REFERENCES

[1] Thomas, W. M. & Nicholas, E. D., (1997), Friction stir welding for the transportation industries, *Materials & Design*, vol.18, no. 4/6, p. 269-273.

[2] Palanivel, R. & Mathews, P.K., (2012), Prediction and optimization of process parameter of friction stir welded AA5083-H111 aluminum alloy using response surface methodology, *J. Cent. South Univ.,* vol. 19, p.1−8.

[3] Shigematsu, I., Kwon, Y.J., Suzuki, K., Imai, T., & Saito, N., (2003), Joining of 5083 and 6061 aluminum alloys by friction stir welding, *Journal of Materials Science Letters*, vol. 22, p. 353– 356.

[4] Yousif, Y. K., Daws, K. M., & Kazem, B. I., (2008), Prediction of friction stir welding characteristic using neural network, *Jordan Journal of Mechanical and Industrial Engineering,* Vol. 2, no. 3, p.151 – 155.

[5] Zhu X.K. & Chao, Y.J., (2004), Numerical simulation of transient temperature and residual stress in friction stir welding of 304 L stainless steel, *Journal of Materials Processing Technology*, vol. 146, p. 263-272.

[6] Meran, C., (2006), The joint properties of brass plates by friction stir welding, *Materials and Design*, vol. 27, p. 719–726.

[7] Cavaliere, P., Nobile, R., Panella, F.W. & Squillace, A., (2007), Mechanical and microstructural behaviour of 2024–7075 aluminium alloy sheets joined by friction stir welding, *International Journal of Machine Tools & Manufacture*, vol. 46, p. 588–594.

[8] Dressler, U., Biallas, G. & Mercado, U.A., (2009), Friction stir welding of titanium alloy TiAl6V4 to aluminium alloy AA2024-T3, *Materials Science and Engineering A*, vol. 526, p. 113–117.

[9] Kostika, A., Coelho, R.S., dos Santos J. & Pyzalla, A.R., (2009), Microstructure of friction stir welding of aluminium alloy to magnesium alloy, *Scripta Materialia*, vol. 60, p. 953–956.

[10] Bagheri, A., Azdast, T. & Doniavi A., (2013), An experimental study on mechanical properties of friction stir welded ABS sheets, *Materials and Design*, vol. 43, p. 402–409.

[11] Mishra, R.S. & Ma, Z.Y., (2005), Friction stir welding and processing, *Materials Science and Engineering R*, vol. 50 p. 1–78.

[12] Threadgill, P.L., (1999), Friction Stir Welding State of the Art, *TWI Report 678*.

[13] Han, M-S., Lee, S-J., Park, J-C., Ko, S-C., Woo, Y-B., & Kim, S-J., (2009), Optimum condition by mechanical characteristic evaluation in friction stir welding for 5083-O Al alloy, *Trans. Nonferrous Met. Soc. China*. Vol. 19, p.17-22.

[14] Sua, J-Q., Nelson, T.W. & Sterling, C.J., (2005), Microstructure evolution during FSW/FSP of high strength aluminum alloys, *Materials Science and Engineering A,* no. 405, p. 277–286.

[15] Vural, M., Ogur, A., Cam G. & Ozarpa, C., (2007), On the friction stir welding of aluminium alloys EN AW 2024-0 and EN AW 5754-H22, *International Scientific Journal*, vol. 28, no. 1, p. 49-54.

[16] Moreira, P.M.G.P., Santos, T., Tavares., S.M.O., Richter-Trummer, V., Vilaça, P. & de Castro, P.M.S.T., (2009), Mechanical and metallurgical characterization of friction stir welding joints of AA6061-T6 with AA6082-T6, *Materials and Design*, vol. 30, p. 180–187.

[17] Ghosh, M., Kumar, K., Kailas, S.V., & Ray, A.K., (2010), Optimization of friction stir welding parameters for dissimilar aluminum alloys, *Materials and Design*, vol. 31. P. 3033–3037.

[18] Dickerson, T. L., & Przydatek, J., (2003), Fatigue of friction stir welds in aluminum alloys that contain root flaws, *Int. J. Fatigue*, vol. 25, p.1399–1409.

[19] Bahemmat, P., Haghpanahi, M., Besharati, M.K., Ahsanizadeh S. & Rezaei, H., (2010), Study on mechanical, micro-, and macrostructural characteristics of dissimilar friction stir welding of AA6061-T6 and AA7075-T6, *Proceedings of the Institution of Mechanical Engineers, Part B: Journal of Engineering Manufacture*, vol. 224, p.1854.

[20] Meilinger, A. & Torok, I., (2013), The Importance of Friction Stir Welding Tool, *Production Processes and Systems*, vol. 6, no. 1, p. 25-34.

[21] Colligan K., (1999), Material Flow Behaviour during Friction Stir Welding of Aluminum, *Supplement to the Welding Journal*, p. 229-237.

[22] Fujii, H., Cui, L., Maeda, M. & Nogi K., (2006), Effect of tool shape on mechanical properties and microstructure of friction stir welded aluminum alloys, *Materials Science and Engineering A*, vol. 419, p. 25–31.

[23] Klobcar, D., Kosec, L., Pietras, A., & Smolej, (2012), A. Friction-Stir Welding Of Aluminium Alloy 5083, *Materials And Technology*, vol. 46, no. 5, p. 483–488.

[24] Heidarzadeh, A., Khodaverdizadeh, H., Mahmoudi, A. & Nazarene, E., (2012), Tensile behaviour of friction stir welded AA 6061-T4 aluminum alloy joints, *Materials and Design*, vol. 37, p.166–173.

[25] Dinaharan, I., Kalaiselvan, K., Vijay, S.J. & Raja, P., (2012), Effect of material location and tool rotational speed on microstructure and tensile strength of dissimilar friction stir welded aluminum alloys, *Archives of civil and mechanical engineering*, vol.12, p. 446 – 454.

[26] Lee, W-B., Yeon, Y-M., & Jung, S-B., (2003), The joint properties of dissimilar formed Al alloys by friction stir welding according to the fixed location of materials, *Scripta Materialia*, vol. 49, p. 423–428.

[27] Amancio-Filho, S.T., Sheikhi, S., dos Santos, J.F. & Bolfarini, C., (2008), Preliminary study on the microstructure and mechanical properties of dissimilar friction stir welds in aircraft aluminium alloys 2024-T351 and 6056-T4, *Journal of materials processing technology*, vol. 206, p. 132–142.

[28] Rao, D., Huber, K., Heerens, J., dos Santos, J.F. & Huber, N., (2013), Asymmetric mechanic al properties and tensile behaviour prediction of aluminium alloy 5083 friction stir welding joints, *Materials Science & Engineering A*, vol. 565, p. 44 –50.

[29] Cavaliere, P., Squillace, A., & Panella, F. (2008), Effect of welding parameters on mechanical and microstructural properties of AA6082 joints produced by friction stir welding, *Journal of materials processing technology*, vol. 200, p. 364–372.

[30] Thamizhmanii, S., Sukor, M.A., & Sulaiman, (2013), Solid state friction stir welding (FSW) on similar and dissimilar metals, *Proceedings of the World Congress on Engineering*, vol. 3.

[31] Costa, J.D., Ferreira, J.A.M., Borrego, L.P., & Abreu, L.P., (2012), Fatigue behaviour of AA6082 friction stir welds under variable loadings, *International Journal of Fatigue*, vol. 37, p. 8–16.

[32] El-Danaf, E.A. & El-Rayes, M.M., (2013), Microstructure and mechanical properties of friction stir welded 6082 AA in as welded and post weld heat treated conditions, *Materials and Design*, vol. 46, p. 561–572.

[33] Babu, S., Ram, G.D.J., Venkitakrishnan, P.V., Reddy, G.M. & Rao, K.P., (2012), Microstructure and Mechanical Properties of Friction Stir Lap Welded Aluminum Alloy AA2014, *J. Mater. Sci. Technol.*, vol. 28, no. 5, p. 414–426.

[34] Ahmed, M.M.Z., Wynne, B.P., Rainforth, W.M., Threadgill, P.L., Wynne, B.P., Rainforth, W.M. & Threadgill, P.L., (2012), Microstructure, crystallographic texture and mechanical properties of friction stir welded AA2017A, *Materials Characterization*, vol. 64 p. 107–117.

[35] Dong, P., Li, H., Sun, D., Gong, W. & Liu, J., (2013), Effects of welding speed on the microstructure and hardness in friction stir welding joints of 6005A-T6 aluminum alloy, *Materials and Design*, vol. 45, p. 524–531.

[36] Yoon, S-O., Kang, M-S., Nam, H-B., Kwon, Y-J., Hong, S-T., Kim, J-C., Lee, K-H., Lim, C-Y. & Seo, J-D., (2012), Friction stir butt welding of A5052-O aluminum alloy plates, *Trans. Nonferrous Met. Soc. China*, vol. 22, p. 619−623.

[37] Peel, M., Steuwer, A., Preuss, M. & Withers, P.J., (2003), Microstructure, mechanical properties and residual stresses as a function of welding speed in aluminium AA5083 friction stir welds, *Acta Materialia*, vol. 51, p. 4791–4801.

[38] Gaafer, A.M. Mahmoud, T.S. & Mansour, E.H., (2010), Microstructural and mechanical characteristics of AA7020-O Al plates joined by friction stir welding, *Materials Science and Engineering A*, vol. 527, p.7424–7429.

[39] Karthikeyan, L., Puviyarasan, M., Kumar S.S. & Balamugundan, B., (2012) Experimental studies on friction stir welding of AA2011 and AA6063 aluminium alloys, *International Journal of Advanced Engineering Technology*, vol. 3, no. 4, p. 144-145.

[40] Khodir, S.A. & Shibayanagi, T., (2008) Friction stir welding of dissimilar AA2024 and AA7075 aluminum alloys, *Materials Science and Engineering B*, vol. 148, p. 82–87.

[41] Hwang, Y.M., Fan, P.L., & Lin, C.H., (2010), Experimental study on Friction Stir Welding of copper metals, *Journal of Materials Processing Technology*, vol. 210, p. 1667–1672.

[42] Aonuma, M. & Nakata, K., (2012), Dissimilar metal joining of ZK60 magnesium alloy and titanium by friction stir welding, *Materials Science and Engineering B*, vol 177, p. 543– 548.

[43] Akinlabi E.T. & Akinlabi, S.A., (2012) Microstructural Characterizations of Dissimilar Friction Stir Welds, *Proceedings of the World Congress on Engineering*, vol. 3.

[44] Uzun, H., Donne, C.D., Argagnotto, A., Ghidini, T., & Gambaro, C., (2005), Friction stir welding of dissimilar Al 6013-T4 To X5CrNi18-10 stainless steel, *Materials and Design*, vol. 26, p. 41–46.

[45] Farias, A., Batalha, G.F., Prados, E.F., Magnabosco, R. & Delijaicov, S., (2013) Tool wear evaluations in friction stir processing of commercial titanium Ti–6Al–4V, *Wear*, vol. 302, p. 1327–1333.

[46] Commin, L., Dumont, M., Masse, J.-E. & Barrallier, L., (2009), Friction stir welding of AZ31 magnesium alloy rolled sheets: Influence of processing parameters, *Acta Materialia*, vol. 57, p. 326–334.

[47] Venkateswarlu, D., Mandal, N. R., Mahapatra M. M. & S. Harsh, P., (2013), Tool Design Effects for FSW of AA7039, *Welding Journal*, vol. 92.

[48] Hao, H.L., Ni, D.R., Huang, H., Wang, D., Xiao, B.L., Nie Z.R. & Ma, Z.Y., (2013), Effect of welding parameters on microstructure and mechanical properties of friction stir welded Al–Mg–Er alloy, *Materials Science & Engineering A*, vol. 559, p. 889–896.

[49] Sharma, C., Dwivedi, D.K. & Kumar, P., (2013), Effect of post weld heat treatments on microstructure and mechanical properties of friction stir welded joints of Al–Zn–Mg alloy AA7039, *Materials and Design*, vol. 43, p. 134–143.

[50] Palanivel R., & Mathews, P.K., (2012), Prediction and optimization of process parameter of friction stir welded AA5083- H111 aluminum alloy using response surface methodology, *J. Cent. South Univ*., vol. 19, p. 1−8.

[51] Parida, B., Mohapatra, M., Biswas, P. & Mandal, N.R., (2012), Study of Mechanical and Micro-structural Properties of Friction Stir Welded Al-Alloy, *International Journal of Emerging Technology and Advanced Engineering*, vol. 2, p. 307-312.

[52] Liang, X-P., Li H-Z., Li, Z., Hong, T., Ma, B., Liu S-D. & Liu, Y., (2012), Study on the microstructure in a friction stir welded 2519-T87 Al alloy, *Materials and Design*. Vol. 35, p. 603–608.

[53] Zhang, L., Shude, Luan, G. & Dong, C., (2011), Friction stir welding of Al alloy thin plate by rotational tool without pin, *J. Mater. Sci. Technol*, vol. 27, no. 7, p. 647-652.

[54] Ren, S.R., Ma Z.Y. & Chen, L.Q. (2007), Effect of welding parameters on tensile properties and fracture behaviour of friction stir welded Al–Mg–Si alloy, *Scripta Materialia*, vol. 56, p.69–72.

[55] Wei, S., Hao C., & Chen, J., (2007), Study of friction stir welding of 01420 aluminum–lithium alloy, *Materials Science and Engineering A*, vol. 452–453, p. 170–177.

[56] Marzoli, L.M., Strombeck, A.V., Dos Santos, J.F., Gambaro C. & Volpone, L.M., (2006), Friction stir welding of an AA6061/Al2O3/20p reinforced alloy, *Composites Science and Technology,* vol. 66, p. 363–371.

[57] Cavaliere, P., Campanile, G., Panella, & F. Squillace, A., (2006), Effect of welding parameters on mechanical and microstructural properties of AA6056 joints produced by Friction Stir Welding, *Journal of Materials Processing Technology*, vol. 180, p. 263–270.

[58] Venkateswaran P. & Reynolds, A.P., (2012), Factors affecting the properties of Friction Stir Welds between aluminum and magnesium alloys, *Materials Science and Engineering A*, vol. 545, p. 26 – 37.

[59] Dinaharana, I., Kalaiselvan, K., Vijaya, S.J. & Raja, P. (2012), Effect of material location and tool rotational speed on microstructure and tensile strength of dissimilar friction stir welded aluminum alloys, *Archives of civil and mechanical engineering*, vol.12, p. 446–454.

[60] Koilraj, M., Sundareswaran, V., Vijayan S. & Rao, S.R.K., (2012), Friction stir welding of dissimilar aluminum alloys AA2219 to AA5083 – Optimization of process parameters using Taguchi technique, *Materials and Design*, vol. 42, p. 1–7.

[61] Wei, L.X., Da-tong, Z. Cheng Q. & Wen, Z., (2012) Microstructure and mechanical properties of dissimilar pure copper/1350 aluminum alloy butt joints by friction stir welding, *Trans. Nonferrous Met. Soc. China*, vol. 22, p. 1298-1306.

[62] Ogura, T., Saito, Y., Nishida, T., Nishida, H., Yoshida, T., Omichi, N., Fujimoto M. & Hirose, A., (2012), Partitioning evaluation of mechanical properties and the interfacial microstructure in a friction stir welded aluminum alloy/stainless steel lap joint, *Scripta Materialia*, vol. 66, p. 531–534.

[63] Kumbhar N. T. & Bhanumurthy, K., (2012), Friction Stir Welding of Al 5052 with Al 6061 Alloys, *Journal of Metallurgy*, p. 1-7.

[64] Wei, Y., Li, J., Xiong, J., Huang, F., Zhang F. & Raza, S.H., (2012), Joining aluminum to titanium alloy by friction stir lap welding with cutting pin, *Materials Characterization*, vol. 71, p. 1–5.

[65] Xue, P., Ni, D.R., Wang, D., Xiao B.L. and Ma, Z.Y., (2011), Effect of friction stir welding parameters on the microstructure and mechanical properties of the dissimilar Al–Cu joints, *Materials Science and Engineering A*, vol. 528, p. 4683–4689.

[66] Esmaeili, A., Givia M.K.B. & Rajani, H.R.Z., (2011), A metallurgical and mechanical study on dissimilar Friction Stir welding of aluminum 1050 to brass (CuZn30), *Materials Science and Engineering A*, vol. 528, p. 7093– 710.

[67] Bahemmat, P. Haghpanahi, M. Besharati, M.K. Ahsanizadeh, S. & Rezaei, H. (2010), Study on mechanical, micro-, and macrostructural characteristics of dissimilar friction stir welding of AA6061-T6 and AA7075-T6g, *Proceedings of the Institution of Mechanical Engineers, Part B: Journal of Engineering Manufacture*, vol. 224, p.1854.

[68] Saeid, T., Abdollah-zadeh A. & Sazgari, B., (2010), Weldability and mechanical properties of dissimilar aluminum–copper lap joints made by friction stir welding, *Journal of Alloys and Compounds*, vol. 490, p. 652–655.

[69] Brown, R., Tang, W. & Reynolds, A.P., (2009), Multi-pass friction stir welding in alloy 7050-T7451: Effects on weld response variables and on weld properties, *Materials Science and Engineering A*, vol. 513–514, p. 115–121.

[70] Tanaka, T., Morishige T. & Hirata, T., (2009), Comprehensive analysis of joint strength for dissimilar friction stir welds of mild steel to aluminum alloys, *Scripta Materialia*, vol. 61, p. 756–759.

[71] Kwon, Y.J., Shigematsu, I. & Saito, N., (2008), Dissimilar friction stir welding between magnesium and aluminum alloys, *Materials Letters*, vol. 62, p. 3827–3829.

[72] Cavaliere, P., De Santis, A., Panella, F. & Squillace, A., (2009), Effect of welding parameters on mechanical and microstructural properties of dissimilar AA6082–AA2024 joints produced by friction stir welding, *Materials and Design*, vol. 30, p. 609–616.

[73] Khodir S.A. & Shibayanagi, T., (2007), Dissimilar Friction Stir Welded Joints between 2024-T3 Aluminum Alloy and AZ31 Magnesium Alloy, *Materials Transactions*, vol.48, no. 9, p. 2501-2505.

[74] Steuwer, A., Peel, M.J. & Withers, P.J., (2006), Dissimilar friction stir welds in AA5083–AA6082: The effect of process parameters on residual stress, *Materials Science and Engineering A*, vol. 441, p. 187–196.

[75] Prime, M.B., Herold, T.G., Baumann, J.A., Lederich, R.J., Bowden, D.M. & Sebring, R.J., (2006), Residual stress measurements in a thick, Dissimilar aluminum alloy friction stir weld, *Acta Materialia*, vol. 54, p. 4013–4021.

[76] Jiang W.H. & Kovacevic, R., (2004), Feasibility study of friction stir welding of 6061-T6 aluminium alloy with AISI 1018 steel, *Proceedings of the Institution of Mechanical Engineers B: Journal of Engineering Manufacture*, vol. 218, no. 10, p. 1323–1331.

[77] Ouyang J.H. & Kovacevic, R., (2002), Material Flow and Microstructure in the Friction Stir Butt Welds of the Same and Dissimilar Aluminum Alloys, *Journal of Materials Engineering and Performance*, vol. 11, no.1, p.2.

[78] Madhusudhan, R., Sarcar, M.M.M., Ramanaiah N. & Rao, K.P., (2012), An experimental study on the effect of experimental parameters on mechanical and microstructural properties of dissimilar aluminium alloy FS welds, *International Journal of Modern Engineering Research*, vol.2, no.4, p.1459-1463.

[79] Khodaverdizadeh H., Heidarzadeh, A. & Saeid, T., (2013), Effect of tool pin profile on microstructure and mechanical properties of friction stir welded pure copper joints, *Materials and Design*, vol. 45, p. 265–270.

[80] Liu, D., Xin, R., Zheng, X., Zhou Z. & Liu, Q., (2013), Microstructure and mechanical properties of friction stir welded dissimilar Mg alloys of ZK60–AZ31, *Materials Science & Engineering A*, vol. 561, p. 419–426.

[81] Choi, D-H., Kim S-K., & Jung, S-B. (2013), The microstructures and mechanical properties of friction stir welded AZ3 with C_aO Mg alloys, *Journal of Alloys and Compounds*, vol. 554, p. 162–168.

[82] Wang, J., Yuan, W., Mishra R.S. & Charit, I., (2013), Microstructure and mechanical properties of friction stir welded oxide dispersion strengthened alloy, *Journal of Nuclear Materials*, vol. 432, p. 274–280.

[83] Galvão, I., Leal, R.M., Rodrigues D.M. & Loureiro, A., (2013), Influence of tool shoulder geometry on properties of friction stir welds in thin copper sheets, *Journal of Materials Processing Technology*, vol. 213, p. 129–135.

[84] Esmailzadeh, M., Shamanian, M., Kermanpur A. & Saeid, T., (2013), Microstructure and mechanical properties of friction stir welded lean duplex stainless steel, *Materials Science & Engineering A*, vol. 561, p. 486–491.

[85] Ahn, B.W., Choi, D.H., Kim, D.J. & Jung, S.B., (2012), Microstructures and properties of friction stir welded 409L stainless steel using Si3N4tool, *Materials Science and Engineering A*, vol. 532, p. 476– 479.

[86] Khodir, S.A., Morisada, Y., Ueji R. & Fujii, H., (2012), Microstructures and mechanical properties evolution during friction stir welding of SK4 high carbon steel alloy, *Materials Science & Engineering A*, vol. 558, p. 572–578.

[87] Sato, Y.S., Nagahama, Y., Mironov, S., Kokawa, H., Hwan, S. ,Park C. & Hirano, S. (2012) Microstructural studies of friction stir welded Zircaloy-4, *Scripta Materialia*, vol. 67, p. 241–244.

[88] Jafarzadegan, M., Feng, A.H., Abdollah-zadeh, A., Saeid, T. Shen J. & Assadi, H., (2012), Microstructural characterization in dissimilar friction stir welding between 304 stainless steel and ST37 steel, *Materials Characterization*, vol. 74, p. 28–41.

[89] Chung, Y.D., Fujii, H., Ueji, R. & Tsuji, N., (2010), Friction stir welding of high carbon steel with excellent toughness and ductility, *Scripta Materialia*, vol. 63, p. 223–226.

[90] Saeid, T., Abdollah-zadeh, A., Assadi H. &Ghaini, F.M., (2008), Effect of friction stir welding speed on the microstructure and mechanical properties of a duplex stainless steel, *Materials Science and Engineering A*, vol. 496, p. 262–268.

[91] Barlas Z. & Uzun, H., (2008), Microstructure and mechanical properties of friction stir butt welded dissimilar Cu/CuZn30 sheets, *Journal of Achievements in Materials and Manufacturing Engineering,* vol. 30, no. 2, p. 182-186.

[92] Cui, L., Fujii, H., Tsuji N. & Nogi, K., (2007), Friction stir welding of a high carbon steel, *Scripta Materialia*, vol. 56, p. 637–640.

[93] Rodrigues, D.M., Loureiro, A., Leitao, C., Leal, R.M., Chaparro, B.M., & Vilaça, P., (2009), Influence of friction stir welding parameters on the microstructural and mechanical properties of AA 6016-T4 thin welds, *Materials and Design,* vol. 30, p. 1913-1921.

[94] Rai, R., De, A., Bhadeshia H.K.D.H. & Debroy, T. (2011), Review: friction stir welding tools, *Science and Technology of Welding and Joining,* vol. 16, no. 4, p. 325.

[95] Bisadi, H., Tavakoli, A., Sangsaraki, M.T. & Sangsaraki, K.T., (2013), The influences of rotational and welding speeds on microstructures and mechanical properties of friction stir welded Al5083 and commercially pure copper sheets lap joints, *Materials and Design*, vol. 43, p. 80–88.

[96] Nandan, R., DebRoy T. & Bhadeshia, H.K.D.H., (2008), Recent Advances in Friction Stir Welding Process, Weldment Structure and Properties, *Progress in Materials Science,* vol. 53, p. 980-1023.